

Journal of Biomedical Optics

BiomedicalOptics.SPIEDigitalLibrary.org

Tailoring the interplay between electromagnetic fields and nanomaterials toward applications in life sciences: a review

Pablo del Pino

Tailoring the interplay between electromagnetic fields and nanomaterials toward applications in life sciences: a review

Pablo del Pino*

CIC biomaGUNE, Biofunctional Nanomaterials Unit, Paseo Miramon 182, 20009 San Sebastian, Spain

Abstract. Continuous advances in the field of bionanotechnology, particularly in the areas of synthesis and functionalization of colloidal inorganic nanoparticles with novel physicochemical properties, allow the development of innovative and/or enhanced approaches for medical solutions. Many of the present and future applications of bionanotechnology rely on the ability of nanoparticles to efficiently interact with electromagnetic (EM) fields and subsequently to produce a response via scattering or absorption of the interacting field. The cross-sections of nanoparticles are typically orders of magnitude larger than organic molecules, which provide the means for manipulating EM fields and, thereby, enable applications in therapy (e.g., photothermal therapy, hyperthermia, drug release, etc.), sensing (e.g., surface plasmon resonance, surface-enhanced Raman, energy transfer, etc.), and imaging (e.g., magnetic resonance, optoacoustic, photothermal, etc.). Herein, an overview of the most relevant parameters and promising applications of EM-active nanoparticles for applications in life science are discussed with a view toward tailoring the interaction of nanoparticles with EM fields. © The Authors.

Published by SPIE under a Creative Commons Attribution 3.0 Unported License. Distribution or reproduction of this work in whole or in part requires full attribution of the original publication, including its DOI. [DOI: [10.1117/1.JBO.19.10.101507](https://doi.org/10.1117/1.JBO.19.10.101507)]

Keywords: functional nanomaterials; electromagnetic fields; nanomedicine; therapy; sensing; imaging.

Paper 140152SSR received Mar. 6, 2014; revised manuscript received May 25, 2014; accepted for publication Jun. 10, 2014; published online Jul. 10, 2014.

1 Introduction

Nanoparticles, in the following referred to as NPs, exhibit outstanding physicochemical properties in contrast to their bulk counterparts, i.e., non-nanostructured materials. Indeed, NPs can be considered as fundamentally new materials owing to distinct size-dependent properties, which some materials present in the size range of ca. 1 to 200 nm. In the nanoscale, properties such as size, shape, and crystallinity can dramatically affect the optical, magnetic, and/or catalytic properties of NPs. In general, the spatial confinement of electrons, phonons, and electric fields in and around the NPs determine most of these novel “nano” properties.¹ Control of the NP properties allows us to anticipate their response to electromagnetic (EM) fields of a particular frequency and intensity. For instance, the optical properties of noble metal² and semiconductor³ NPs and the magnetic properties of ferrite NPs⁴ can be tailored by changing both their size and shape.

The cross-sections of NPs are typically orders of magnitude larger than those of organic molecules, and thus, absorption and scattering processes are key for certain applications.⁵ Metallic NPs are, for instance, much more efficient scatterers ($>10^6$ -fold) than any organic molecule. Clearly, this has important implications in the context of biomedical applications, which are based on the response of materials to EM fields. Moreover, current synthetic bottom-up approaches allow for tailoring the interaction of NPs with a specific EM field by simply adjusting the composition, size, and shape.^{6,7} NPs can thus be engineered for a specific application. For example, NPs aimed at deep body imaging have to absorb and emit in the so-called

biological window in the near-infrared (NIR), i.e., in the wavelength range of 800 to 1100 nm. Otherwise, both excitation and detection of the signal would be impaired due to scattering by the surrounding physiological components. For the case of noble metal NPs and quantum-dots (QDs), these optical features can be achieved by increasing the anisotropy of the NPs (e.g., nanorods, nanoprisms, nanostars, etc.)⁶ and by controlling the composition and diameter of the QDs,³ respectively. In the biological window, EM fields interact minimally with physiological components, such as blood, water, and fat.⁸ Quoting the words of Kotov: “the only way is up,” which makes reference to the tunability of the optical properties in the NIR of upconverting nanoparticles (UCNPs) for bioimaging.⁹

Bioimaging using shortwave infrared (SWIR) light with wavelengths from 0.9 to 1.7 microns represents another recent example in this direction. The recent development of indium gallium arsenide sensors has made SWIR imaging technically possible. Likewise, NIR and SWIR bioimaging benefit NPs, which can interact efficiently with these wavelengths.^{10–12}

In the following, some important parameters and relevant examples with regard to EM-active NPs will be discussed. The definitions of NPs and nanomaterials are relatively broad, and thus, to simplify, this review will focus on (1) colloidal NPs based on inorganic materials and (2) some relevant bioapplications with regard to the interaction of NPs with EM fields, i.e., bioapplications based on EM-active NPs. Please forgive me for the important omissions, as there will be plenty due to the wide scope of this topic. This review is intended for non-specialists in any specific bioapplication of NPs. I hope it will provide an ample overview about the opportunities that EM-active NPs can offer in life science applications.

*Address all correspondence to: Pablo del Pino, E-mail: pdelpino@cicbiomagune.es

2 Biological Performance by Chemical Design

Understanding the interplay between engineered NPs immersed in physiological environments and EM radiation is a complex issue that requires multidisciplinary teams in order to achieve relevant research developments. The best NPs in terms of physical properties might be useless for a specific bioapplication if they are toxic, unstable in physiological media, or covered by proteins nonspecifically,¹³ to mention just a few aspects. Nanotoxicology,¹⁴ functionalization of NPs with biomolecules,¹⁵ the protein corona,¹⁶ avoiding sequestration of NPs by the immune system,¹⁷ or using biocompatible EM fields,³ among others, are trending issues, which will surely determine the spread of bionanotechnology in the near future.

Two main aspects are critical toward the design of such functional NPs. First, the chemical design of the inorganic core needs to be optimized. The interaction between EM fields and NPs can be finely tailored by controlling NPs' properties, such as size, shape, structure, and composition.³ While the inorganic material should act as an antenna, the fields should not affect the surrounding biological environment. EM-active NPs should also convert the absorbed or scattered EM fields into a specific response, such as fluorescence, field enhancement, nanoheating, etc. Second, the surface of these materials needs to be engineered to produce stable colloids in physiological media.¹³ That is, surface modifications are typically required to warrant long-term stability, prevent corrosion, preserve the original physical properties, etc. NPs can be further derivatized into biologically active NPs by surface modification with molecules of biological relevance, which confer additional features such as targeting capabilities, cell internalization features, prolonged circulation time, invisibility to the immune system, etc. The composition and thickness of the organic coating are also crucial as it forms the interphase between NPs and the environment, including ions, cells, proteins, tissue, etc.¹⁸ Please notice that the organic coatings might be intended (by design) or accidental, for example, due to the adsorption of proteins, which forms the so-called protein corona.¹⁶ Therefore, the coating may interfere with the NP's response via thermal isolation, or quenching, enhancement or transfer of fluorescence, etc. One example in this direction is nanoheating by NPs. Theoretical calculations have shown that the heat produced by one single NP affects only the most immediate vicinity of the NP by thermal diffusion.¹⁹ Thus, as heat diffusion is confined within few nanometers from the NP's surface, thick organic coatings will impede heating a target in the cellular membrane. Likewise, the protein corona has been reported as the prime target of such single NP heating, which may affect the biological fate of such a system *in vivo*.²⁰ Not only nanoheating but also Raman and fluorescence signals can be affected by the physiological environment and, thereby, the bioperformance of NPs might be compromised. One has to keep in mind that the original design of the NPs can be severely affected by physiological components. Others and I have recently reviewed this topic in detail.^{13,16,18}

3 Biochemistry and Biomolecular Processes Occur at the Nano- and Microscale

In addition to the ability of NPs to interact efficiently with EM fields, the size scale where this interaction occurs is of utmost importance and suitability for biological processes. Being able to remotely manipulate nanomaterials with EM fields opens up a

variety of opportunities in life sciences because biochemistry is actually governed by nano- and microscale processes, such as biomolecular recognition, molecular gradients, signaling pathways, cellular uptake, etc. The ability to control ion channels and neurons through heating of NPs is one remarkable example, which illustrates how EM-active NPs can control biological processes.²¹ Clearly, the size scale in this example is as important as the heating properties of the NPs, i.e., heating is required in the nanoscale only. The Gueroui group has reported other fascinating examples with regard to EM control over cellular fate by using functionalized magnetic NPs,^{22–24} which were able to induce gradients of signaling proteins in the microscale by using magnetic field gradients.

EM-active NPs can be combined with one or more components from a library of molecules of biological relevance, including proteins, peptides, carbohydrates, nucleic acids, peptides, antifouling polymers, etc.^{25,26} The capability to perform more than one simple task is one of the most promising aspects of bionanotechnology, i.e., the so-called multifunctional NPs. The examples in the literature about multifunctional NPs are manifold,^{15,27–31} and the combinations of molecules and NPs are very diverse. Figure 1 schematically depicts several possible functionalities, which are categorized depending on the NPs' design. As previously acknowledged, this review focuses on EM-active NPs, and thus, several NP models and applications will not be discussed. This review will not cover NP models

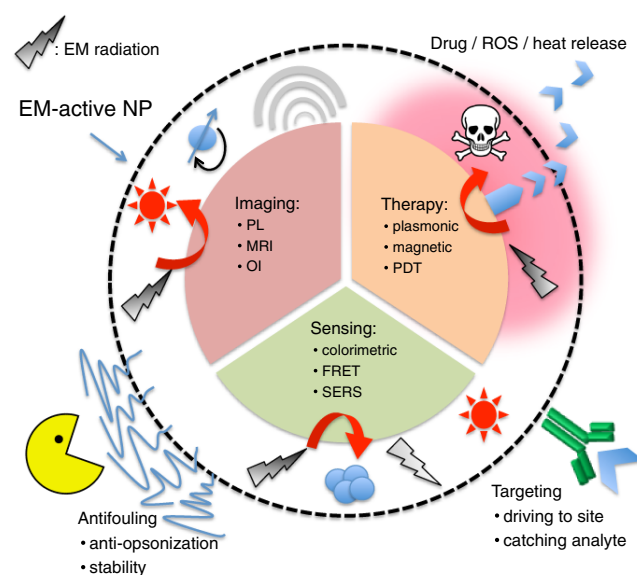


Fig. 1 Schematic representation of three relevant types of active nanoparticles (NPs). The imaging panel represents three possible scenarios, i.e., photoemission, magnetic resonance contrast, and optoacoustic contrast, which can be realized by different types of NPs, including quantum-dots, magnetic NPs, and plasmonic nanomaterials (NMs). The heating panel represents the nanoheating capabilities of plasmonic and magnetic NPs, which upon coupling with light and radiofrequency (RF) radiation, respectively, are able to heat their surroundings, enabling hyperthermia and drug-release applications. The sensing panel depicts several biosensing applications driven by active NPs, such as colorimetric, Förster (fluorescence) resonant energy transfer, and SERS assays. The inner part of this figure (inside the dotted circle) represents the interaction between electromagnetic fields and NPs toward biological applications, whereas the outer part shows important molecules of biological relevance, which upon combination with different NPs (scaffolds) allows diverse range of multifunctionality.

Table 1 Electromagnetic (EM)-active nanoparticles (NPs) and corresponding applications.

	Process	NP models	EM/NP interaction
Imaging	Photoluminescence (PL)	Quantum-dots (QDs) ^{32,33} Upconversion NPs (UCNPs) ³⁴ Metal nanoclusters (NCs) ³⁵	NPs absorb light of certain energy, which depends on the NPs' model (size, shape, composition, etc.), and upon relaxation emit light.
	Optoacoustic (OI)	Noble metal NPs ^{36,37}	NPs absorb light, which typically is in resonance with the NPs' plasmon band; the absorbed energy produces acoustic waves through thermoelastic expansion of the NPs.
	Magnetic resonance (MRI)	Magnetic NPs ³⁸	NPs absorb radiation and produced alterations in magnetic relaxation of the surrounding atoms.
Therapy	Plasmonic heating	Noble metal NPs ³⁹ doped semiconductor NPs ⁴⁰	NPs absorb light, which matches their plasmon band; the absorbed energy is transferred to the crystal lattice of the NPs, which upon relaxation get hot. Heating in the nanoscale occurs by thermal diffusion.
	Magnetic heating	Magnetic NPs ⁴¹	The magnetic moment of magnetic NPs couples to alternating magnetic fields of radiofrequency radiation; upon magnetic reversal, the absorbed energy is dissipated in the form of heat.
	Photodynamic	UCNPs ⁴²	NPs absorb more than one photon, which triggers the emission of one photon at higher energy by anti-Stokes emission.
Sensing	Optical readout	Noble metal NPs ⁴³⁻⁴⁵	The optical, magnetic, or electric properties of NPs are affected by the detection of the analyte. In general, the NPs are modified with biomolecules, which can recognize a specific analyte. The actual change in these properties is related to the amount of analyte.
	Magnetic readout	Magnetic NPs ⁴⁶	
	Electric readout	Noble metal, carbon nanotubes (CNTs) ^{47,48}	

whose imaging, therapeutic, or sensing features are based on organic ligands/components, such as purely organic nanostructured materials, NPs as carriers of functional molecules, etc. As summarized in Table 1, three different categories of EM-active NPs will be considered, i.e., imaging, therapeutic, and biosensing agents.

The range of functions provided to NPs by molecules can be as broad as the diversity of molecules. Therefore, and for the sake of simplicity, the molecules typically used to add

biofunctionality(ies) to NPs could be categorized according to three main functions, i.e., targeting, antifouling, and treatment with drugs. Table 2 summarizes some of the most widely used molecules in combination with NPs.

In the literature, there are plenty of examples about multifunctional NPs designed to perform complex tasks simultaneously, using plasmonic,⁷⁶ upconversion,⁷⁷ semiconductor,⁷⁸ or magnetic⁷⁹ EM-active NPs as scaffolds upon which a diverse range of multifunctionality can be built. Furthermore, many

Table 2 Molecules of biological relevance typically used in combination with NPs.

	Molecule	Function	Examples
Targeting	Antibodies	Labeling of organelles and cellular components, sensing	QDs ⁴⁹ , magnetic NPs, ⁵⁰ metallic NPs ⁴⁵
	Carbohydrates	Lectin-carbohydrate interactions, sensing, cellular uptake	QDs, ⁵¹ metallic NPs ⁵² , magnetic NPs ⁵³
	Lipoproteins	Cancer imaging and therapy, ⁵⁴ Alzheimer's treatment ⁵⁵	Polymeric NPs
	Hormones	Target hormone-receptors in cancer	Au NPs, ⁵⁶ CNTs ⁵⁷
	Folate	Cancer imaging and therapy	UCNPs, ⁵⁸ magnetic NPs, ⁵⁹ Au NPs ⁶⁰
Antifouling	PEG	To prevent unspecific interaction with plasma proteins, which ultimately leads to sequestration by the immune system	Metallic, ⁶¹ magnetic, ⁵³ semiconductor, ⁶² upconversion NPs ⁶³
	Zwitterionic ligands		Au NPs, ⁶⁴ silica NPs ⁶⁵
Drugs	Nucleic acids	Gene therapy, sensing	Magnetic, ^{66,67} Au NPs ^{43,68-73}
	Chemotherapeutics	Cancer treatment	Magnetic, ⁷⁴ Au, ⁷⁵ upconversion NPs, ⁵⁸ QDs ²⁸

Table 3 Theranostic EM-active NPs.

	Imaging modality	Therapy modality	Targeting	Examples
Magnetic NPs	MRI	Hyperthermia/chemotherapy	Magnetic field	Magnetic polymersomes ⁷⁴
	Radionuclide-based/ MRI/PL	siRNA	Human serum albumin coating	Multifunctional NPs ⁸⁰
	PL	siRNA	Magnetic field	Magnetic lipospheres ⁶⁶
QDs	PL/Förster (fluorescence) resonant energy transfer	Chemotherapy	Aptamer-receptor	Multifunctional QDs ²⁸
	PL	Chemotherapy/ siRNA	—	Multifunctional QDs ⁸¹
UCNPs	PL	Chemotherapy	Folate-receptors	Multifunctional UCNPs ⁵⁸
	PL	siRNA photo delivery	—	Multifunctional UCNPs ^{82,83}
	PL/MRI	Photodynamic	—	Multifunctional UCNPs ⁸⁴
Plasmonic NPs	Optoacoustic/MRI/Dark-field	Drug release	—	Au nanoshells ⁸⁵
	Optoacoustic/MRI/PL	Photoablation	Enhance permeability and retention (EPR) effect	Graphene oxide-magnetic NPs ⁸⁶
	Computed tomography	Radiation	EPR effect	Au micelles ⁸⁷
	Optoacoustic/dark-field/multiphoton/PL	Thermo-chemotherapy	EPR effect/surface molecules	Au NPs, carbon nanomaterials, Pd nanosheets, Cu _{2-x} Se ⁸⁸

NP models have been shown to work simultaneously as imaging and therapy agents, that is, multifunctional NPs typically referred to as theranostic probes. As we shall see in the following sections, NP models such as QDs, plasmonic, upconversion, and magnetic NPs can work as therapeutic and imaging agents. Although many of the most promising NP models have been shown to exhibit theranostic features, to simplify, this review will independently treat imaging and therapeutic NPs. Table 3 summarizes some examples of theranostic agents based on EM-active NPs.

4 Nanoimaging

In this section, basic principles and opportunities with regard to the use of NPs as imaging nanoantennas will be discussed. Three main phenomena will be covered, that is, photoluminescence (PL), magnetic resonance imaging (MRI) contrast, and optoacoustic imaging (OI) contrast. Others also exist, such as thermal imaging,^{89,90} Raman mapping,^{91,92} x-ray computed tomography (CT),⁸⁷ radionuclide-based imaging,⁸⁰ or nonlinear optical phenomena, such as two-photon luminescence;⁹³ however, to date, they are less widely spread than the techniques covered herein. Please notice that this review focuses on imaging based on the physicochemical properties of the inorganic core of EM-active NPs and, therefore, imaging techniques based on NPs labeled with organic fluorophores or radio-labeled will not be discussed.

4.1 Photoluminescence

Equivalent to common organic fluorophores, upon absorption of light, various NP models can emit light typically of longer wavelengths. Indeed, the colloidal synthesis of QDs was probably one of the main triggers of the current nanohype. These NPs made of semiconductor materials exhibit extraordinary

fluorescence when they are illuminated at wavelengths intrinsically related to their composition, structure (core or core@-shell), size, and surface chemistry.³ Actually, QDs present several enhanced optical features compared to organic fluorophores, such as size tunability of absorption and emission, high quantum yield, photostability, etc. For a detailed comparison between QDs and common dyes, the reader is referred to the work of Resch-Genger et al.⁵

Since the original works of Brus,⁹⁴ Bawendy,⁹⁵ Alivisatos,⁹⁶ Weller et al.,⁹⁷ and others,^{98,99} tremendous advances have been done with controlling the optoelectronic properties of QDs, that is, how QDs respond to light excitation. These have been achieved mainly by the steady developments in colloidal chemistry, which have enabled one to finely control the size, shape, composition, coating, etc., of QDs. Currently, synthetic methods permit us to choose QDs with almost any emission from the UV to the SWIR.^{100–103} Yet, although QDs are very bright and photostable, their range of application *in vivo* has been traditionally limited due to toxicity concerns. Traditional QDs for *in vivo* imaging contain toxic ions, such as Cd, Hg, Te, Pb, etc., which can be released upon corrosion. Thus, less toxic compositions, such as InP/ZnS, Ag₂S, or CuInS₂/ZnS QDs, have been investigated as alternatives to provide new opportunities in the medical field.¹⁰⁴ Coating methods have also been refined toward limiting the release of toxic ions, preserving the optical properties [high quantum yield (QY)], and enabling the colloidal stability of QDs in aqueous solution.^{105,106}

Carbon nanomaterials, such as nanotubes, graphene, nanodots, and nanodiamonds, can also be used for bioimaging owing to their optical response.^{107,108} However, several aspects, such as cytotoxicity concerns, emission wavelength, or low extinction, which depend on the NP models, currently limit their use for bioimaging purposes.¹⁰⁹

As an alternative to QDs, UCNPs represent a relatively new and exciting type of imaging agent. The upconversion phenomena involve the combined absorption of more than one photon, which triggers the emission of one photon at higher energy by anti-Stoke emission.^{9,10} UCNPs used for bioimaging are typically composed of a host matrix (e.g., Y_2O_3 , Y_2O_2S , LaF_3 , $NaYF_4$, and $NaGdF_4$), doping lanthanide ions (e.g., Er^{3+} , Tm^{3+} , and Ho^{3+} , which are the actual absorbers), and Yb^{3+} for enhancing the emission efficiency. Although the optical properties of UCNPs can be readily tailored by design, there is an important drawback with respect to QDs, that is, very low QY (0.005 to 0.3%).¹¹ This point represents a challenging hurdle as it has a difficult solution due to the low extinction of the lanthanides.

Last in this section, a very new class of fluorescence probes is discussed, that is, fluorescence metal nanoclusters (NCs).¹² NCs are made of few to hundreds of Ag and/or Au atoms (core size <2 nm) capped with molecules, which also importantly affect their optical features.³⁵ In contrast to bulk or NPs made of Au or Ag, the radiative decay of these NCs is very efficient. Indeed, the QY of NCs can be up to nine orders of magnitude larger than QY of the corresponding bulk material. NCs present good photostability in physiological media, high QY (although, in general, smaller than for QDs), broad tunability from the UV to the NIR, and large Stokes shifts.^{113,114} The opportunities that these materials open in the context of bioapplications are manifold; however, much work is still needed with regard to the impact of these materials on physiological environments. Au ions are toxic as Cd or Ag. However, Au NPs are believed to be among the safest NPs since they do not decompose readily because Au is the noblest metal. Clearly, in the case of Au NCs, which have an extreme surface-to-volume ratio, their corrosion behavior and cytotoxicity should be reevaluated. Understanding the biological fate and impact on proteins, organelles, etc., of NCs requires further investigations.

4.2 MRI Contrast

MRI is widely used in the clinic and presents several advantages over other techniques, such as CT or positron emission

tomography, which utilize ionizing radiation. MRI contrast is given by the distinct magnetic relaxation processes of the nuclear spins of hydrogen atoms in water and fat, the major hydrogen-containing components of the human body. Other elements can also be used, including 3He , ^{13}C , ^{19}F , ^{17}O , ^{23}Na , ^{31}P , and ^{129}Xe . MRI is noninvasive, nondestructive, and allows for full-body three-dimensional reconstruction with high spatial resolution and excellent soft tissue contrast.⁴ Nevertheless, MRI as an endogenous technique suffers from poor sensitivity. Therefore, contrast agents, such as gadolinium-complexes and iron oxide NPs, are widely used, enabling superior sensitivity. It should be noted that gadolinium-complexes might release toxic ions and suffer from low circulation time.⁴ Iron oxide NPs are actually used to induce local field inhomogeneities (as nanoantennas) that affect the relaxation time of protons, leading to positive or negative contrast. Indeed, tailoring the size of these NPs from <4 nm to ca. 40 nm can be used to produce distinct effects on the relaxivity, called longitudinal or T_1 , and transversal or T_2 . Furthermore, doping with transition metal ions or clustering of NPs induces very high contrast (in this case via enhancement of T_2). The tunability, biocompatibility, and versatility make iron oxide NPs, in terms of biofunctionalization, a promising candidate for being widely used in the clinic. We refer to the original work of Lee and Hyeon for an extended review of this topic.⁴

4.3 Optoacoustic Imaging

The newest and most exciting technique is discussed last in the imaging section, owing to the simplicity of its principles and the fact that it is based on already developed technologies, i.e., sonography and tomography.¹¹⁵ OI is a hybrid technique that listens to light. The principle relies on detecting acoustic waves upon thermal relaxation of a photoabsorber excited with an intense pulse of NIR light, cf. Fig. 2. The two main advantages are the penetration depth, owing to NIR excitation, and the fact that resolution is not affected by scattering, as it is based on ultrasound. However, sensitivity can be poor due to limited endogenous contrast. Thus, NPs are ideal probes as OI contrast agents, with improved sensitivity, optical tunability by

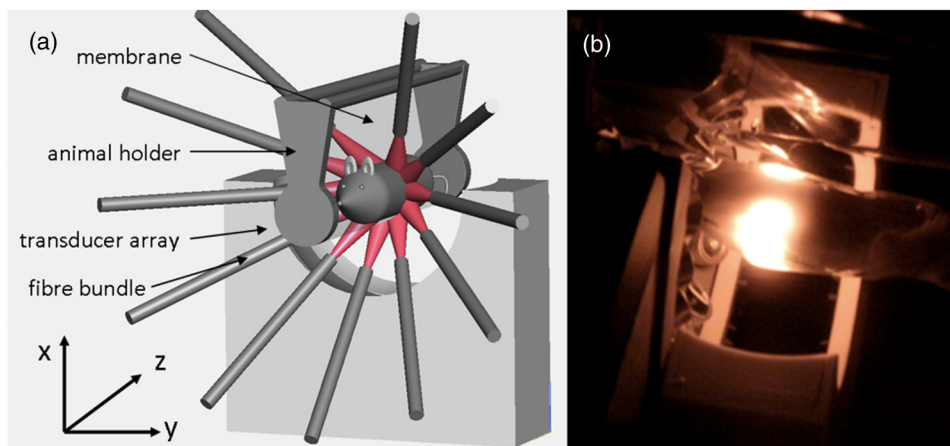


Fig. 2 (a) Schematics of an optoacoustic imaging (OI) system. The slight fiber bundle angle allows illumination of the sample exactly above the transducer array. The animal holder allows the sample to be moved and the recording of sequential slices in precise and predefined steps. (b) OI system used in the work of Bao et al., which reported the OI bioimaging of gastrointestinal cancer by using gold nanoparticles.³⁷ The clear illumination ring on the animal, which is wrapped in a thin transparent plastic foil and placed in a water tank, allows homogeneous light energy to be transferred around the focal point of the transducer array. Reproduced with permission from Ref. 37.

Table 4 Imaging using EM-active NPs.

Imaging modality	NPs model	Examples	Tuning parameters	Pros	Cons
PL	QDs	Ag ₂ S (QY: 15.5%) ¹² CuInS ₂ /ZnS (QY: 20 to 30%) ¹⁰² C-dots (QY: 17%) ¹²² Nanodiamonds (QY: 70%) ¹²³ Si NPs (QY: 60%) ¹²⁴	Size, shape, surface chemistry, structure ³	Fast (<200 ms per frame) ¹²⁵ Sensitivity: picomolar	Spatial resolution (SR: 1 to 3 mm; one recent work ~30 μm) ¹²⁵ Tissue penetration (<1 cm)
	UCNPs	NaYF ₄ : 2% Er ³⁺ , 20% Yb ³⁺ (QY: 0.005 to 0.3%) ¹¹¹	Doping, size ¹²⁶		
	NCs	Au NCs (QY: 2.9%) Au/Ag NCs (QY: 3.4%) Ag _x Au _{25-x} (x = 1 to 13) (QY: 40.1%) ¹²⁷	Size, ligands, doping ¹²⁷		
MRI	T ₂ agents (superparamagnetic and ferrimagnetic NPs)	Fe ₃ O ₄ , MnFe ₂ O ₄ , (Zn _x Mn _{1-x})Fe ₂ O ₄ , Fe/MnFe ₂ O ₄ NPs ⁴	Size, doping, structure, ligands ⁴	SR: ~50 μm Unlimited tissue penetration	Sensitivity: micromolar to nanomolar Slow processing
	T ₁ agents (superparamagnetic and paramagnetic NPs)	Ultrasmall Fe ₃ O ₄ , ¹²⁸ Mn ₃ O ₄ , ¹²⁹ Gd ₂ O ₃ NPs ³⁸			
OI	Metal NPs, carbon nanomaterials	Au nanorods, ³⁶ Au nanoprisms, ³⁷ Au nanocages, ¹¹⁷ Ag nanoprisms, ¹¹⁸ graphene nanosheets, ⁸⁶ CNTs ¹¹⁶	Size, anisotropy, structure ¹¹⁹	SR: ~50 μm Sensitivity: picomolar Fast	Tissue penetration (<5 cm) Still developing

QY, quantum yield.

chemical design, and biotargeting capabilities. To date, carbon nanotubes (CNTs) and anisotropic metal nanoparticles (Au and Ag) have been tested as OI contrast agents with excellent results *in vivo*.^{36,37,116-118} The main requirement of these probes is that they should be able to absorb in the NIR; clearly, materials with highest absorption will produce best contrast.¹¹⁹ Current synthetic methods can be used to synthesize NPs with absorption bands in the range where OI operates. For instance, gold nanoprisms and nanorods,^{37,120} whose plasmon band can be adjusted along the NIR by chemical design, have been used as OI contrast agents. Actually, expanding the excitation sources used by OI into the SWIR will improve the possibilities of this technique owing to deeper tissue penetration.^{3,121}

As summary of the imaging section, Table 4 shows important parameters for the different imaging modalities and selected EM-active NP models.

5 Nanotherapy

Most of the therapeutic uses of NPs, i.e., nanomedicine, are based on loading the NPs with a variety of functional molecules, thereby enabling multifunctional NPs.^{68,130} Cancer treatment

has been one major area where NPs have been extensively applied.¹³¹ Ideally, multifunctional NPs should circulate in the bloodstream undetected by the immune system, reach the targeted region, and release or expose a drug or stimuli. Multifunctional NPs present not only several advantages compared to common therapeutic drugs, such as prolonged circulation time, targeting capabilities, superior stability, and enhanced pharmacokinetics, but also potential theranostic features. The diversity of therapeutic NPs can be as broad as the potential drug molecules that can be loaded on the NPs, including anti-cancer drugs, proteins, and nucleic acids.¹³² Although the therapeutic opportunities of NPs are manifold, this review focuses on EM-active NPs alone, and thus, two main therapeutic processes will be discussed: nanoheating and photodynamic therapy (PDT). The therapeutic gain relies on the interaction of the inorganic core of NPs with EM fields. Although other NP-based therapeutic approaches exist, nanoheating and PDT are among the most widely investigated.

A variety of nanomaterials show great promise as nanoheaters, that is, NPs able to produce heat locally (at its surroundings) upon EM irradiation. In many applications based, for example, on plasmonics or in MRI, nanoheating is actually an unwanted phenomenon.¹³³ Several bioapplications based on nanoheating

using NPs have been mainly developed in the last decade. Applications such as negative index of refraction, focusing and imaging with subwavelength resolution, invisibility cloaks, etc., require low-loss plasmonic materials, i.e., graphene, alkali metals, etc., as alternatives to noble metals, such as Au and Ag, which are indeed excellent for nanoheating.¹³³

The capability of being able to release heat upon remote EM exposure has opened new opportunities for a variety of goals in life sciences. Local heating with colloidal NPs has been used for killing tumoral cells,¹³⁴ drug-release applications,^{135,136} ultralow detection of tumoral markers,⁴⁵ imaging *in vivo*³⁷ and *in vitro*,¹³⁷ or even sterilization.¹³⁸ In the frame of oncological hyperthermia, both magnetic and plasmonic NPs have been investigated as nanoheaters. Either can be remotely activated by radiation that do not or minimally interact with physiological tissues and fluids. Actually, the major challenge concerning colloidal chemistry within this framework resides in being able to produce NPs that absorb in EM regions where tissue absorption remains minimum, i.e., biological windows. Engineered nanomaterials with tailored heating performance, as well as suitable organic coatings, are continuously developed toward more efficient interactions with EM radiation and the performance of more complex tasks in biological environments. As previously discussed, these materials can be used simultaneously as contrast agents by using imaging techniques that rely on their magnetic (e.g., MRI) or plasmonic behavior (e.g., OI), thereby enabling theranostic NPs. Moreover, plasmonic nanoheating can be used in combination with other therapeutic and imaging approaches. Chen, Nie, and coworkers have recently reported on plasmonic nanoheating combined with PDT.⁶³ They proposed a theranostic nanoplatform based on plasmonic photosensitizer-loaded vesicles, which, in addition, can be used as triple-imaging agents, i.e., NIR fluorescence, thermal and photoacoustic

imaging, cf. Fig. 3. Previous works have demonstrated the feasibility of dual imaging-therapeutic NPs based on active NPs by using magnetic and resonant light excitation.^{139,140}

Two main decay processes (heat losses) can be accountable for nanoheating, i.e., magnetic relaxation and plasmonic relaxation. Both are based on the capability of magnetic and plasmonic NPs to couple to the magnetic component of radio-frequency (RF) radiation or the electric component of light, respectively. Thus, local heating can be produced upon dissipation of the absorbed energy.

5.1 Plasmonic Heating

Most relevant plasmonic NPs for nanoheating include noble metals [Au (Ref. 134) and Ag (Ref. 141)], semiconductor NPs [Cu_{2-x}Se,⁴⁰ CuS,¹⁴² and CuTe (Ref. 143)], CNTs,¹³⁹ and graphene nanomaterials.¹⁴⁴ The variety of compositions, sizes (from 10 nm to hundreds of nanometers), and shapes (core-shell, rod-like, cube, star-like, prismatic, triangular, etc.) is remarkable. Their common property is NIR activity. As previously discussed, ideal plasmonic nanoheaters should absorb as much light as possible and they should also exhibit high heating losses (high conductivity). Thus, Au represents an ideal nanoheater, in principle safer than Ag due to toxicity concerns. Ag NPs are more readily oxidized than Au, releasing toxic Ag ions. Therefore, most up-to-date plasmonic nanoheating studies have been carried out with Au anisotropic NPs, such as nanorods¹³⁴ or nanoprisms³⁹, and gold nanoshells.¹⁴⁵

The light-to-heat mechanism involves the resonant absorption of light by the conduction electrons of the NPs, which couple to the incoming radiation. Scattering between the hot electrons and the crystal lattice enables energy dissipation by phonon-phonon scattering. For details about the plasmonic photothermal effect, the reader is referred to an excellent review by

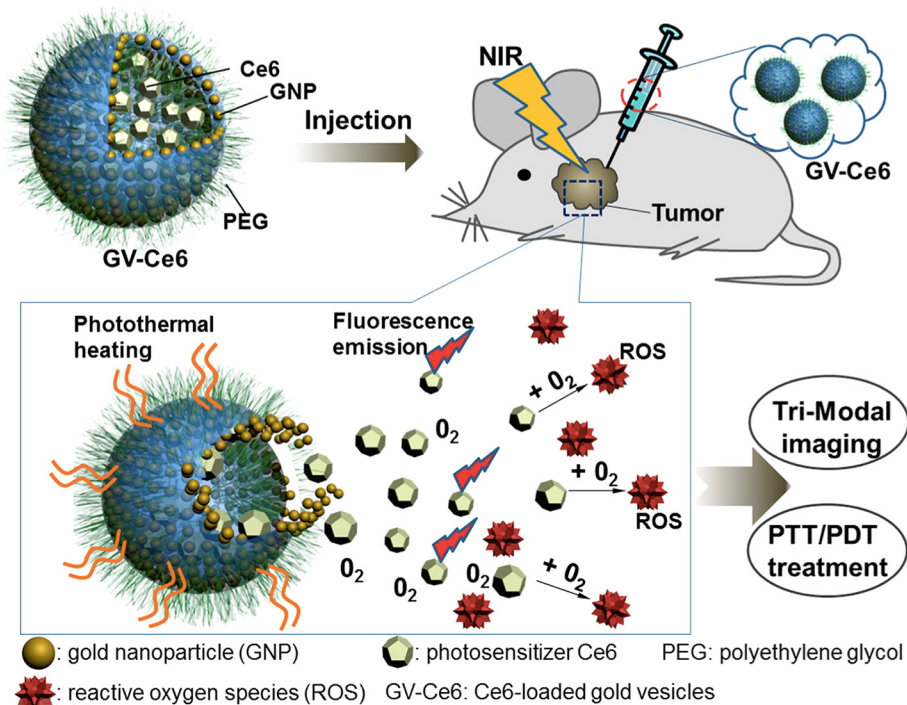


Fig. 3 Theranostic NPs: photosensitizer (Ce6)-loaded plasmonic gold vesicles, which provide trimodal imaging capabilities, i.e., fluorescence, thermal and OI, and photothermal/photodynamic cancer therapy. Reproduced with permission from Ref. 63.

Baffou and Quidant, which discusses many important parameters, including thermal diffusion, continuous or pulse illumination, coupling effects, and thermal confinement, among others.¹⁹

Plasmonic nanoheating therapy has been explored using different approaches, ablation of tumoral cells being the most straightforward and widely reported to date.^{146,147} The use of plasmonic nanoheating for cancer treatment has indeed reached clinical trials (see AuroLase® Therapy). The principle is simple, as it only requires surface modification of the nanoprobes to enable cellular uptake and prolonged circulation time, and a light source. Different biofunctionalization strategies using biomolecules have been reported to date, enabling specific targeting. Though simple, this approach is very powerful, due to the spatiotemporal control of the illumination of the tissue's areas to be destroyed.

Other more elegant approaches employ nanoheating to promote drug release, which can then be used for killing or treating the targeted cells. Halas and coworkers used the nanoheating-release approach by using nanorods and nanoshells.^{136,148–150} In one particularly interesting example, they functionalized the nanoheaters with complementary nucleic acid strands, which upon light excitation can undergo dehybridization of the complementary strand, i.e., the therapeutic drug siRNA, inducing gene silencing.¹³⁶ Other approaches have been employed in organic microparticles (layer-by-layer capsules,¹⁵¹ liposomes,¹⁵² polymer particles,⁷⁵ etc.) functionalized with plasmonic NPs, which upon illumination can undergo a phase transition, enabling the release of the caged drug inside the cells. Parak and coworkers have used plasmonic polyelectrolyte capsules to release different drugs, including polymers,¹⁵³ pH indicators, and proteins,¹⁵⁴ as well as nucleic acids,⁶⁷ inside the cytosol of cells at the level of single cells.

5.2 Magnetic Heating

Another type of nanoheaters involves the coupling of the alternating magnetic field of radio-frequency radiation to the magnetic moment of magnetic NPs. Magnetic dipoles result from the spinning of some of the NP electrons. These polarized electrons can align parallel or antiparallel with respect to the neighboring ones and respond very differently to an applied magnetic field. This, in turn, defines how materials are classified as paramagnets, ferromagnets, ferrimagnets, or antiferromagnets. Falling into one of these categories depends on the size of the material, and thus, the magnetic behavior of a particular material can be tuned by adjusting its size.¹⁵⁵ Indeed, superparamagnetism is intrinsically linked to the nanometer range. In contrast to ferromagnetic and ferrimagnetic (FM) NPs, in the absence of a magnetic field, superparamagnetic (SPM) NPs are not magnetized. This actually prevents magnetic coupling and, subsequently, unwanted agglomeration of NPs. Obviously, magnetic agglomeration should be prevented to preserve the colloidal stability and properties of the materials. This is especially important for biological applications where agglomeration can impede the performance of the nanomaterial. Furthermore, the magnetic dipole of SPM NPs and single-domain small FM NPs can couple to RF radiation using relative low field amplitudes, which enables the heating of their local environment upon energy dissipation. This is the basis of magnetic fluid hyperthermia, a technique investigated for decades in the field of cancer treatment.^{156–160} The pillars of this therapeutical technique are (1) tumors are inherently more susceptible to increased temperatures than healthy tissue; (2) magnetic NPs can produce heat

upon excitation with RF radiation; and (3) the intensity and energy required for exciting these NPs is in a physiological regime, which typically requires frequencies and field amplitudes <1 MHz and 250 G, respectively. Tissue surrounding tumors and nontargeted with NPs will not be damaged upon RF exposure.

Many of the research efforts concerning magnetic hyperthermia have been devoted to the development of NPs with the highest specific absorption rate (SAR), i.e., the capability of the magnetic fluids to absorb and heat as much as possible. There are different models that aim to explain magnetic relaxation processes involved in magnetic heating. Ultimately, the source of nanoheating is the magnetic reversal of the magnetic moment of a single NP.¹⁶¹ Magnetic reversal is actually influenced by several properties, such as magnetic anisotropy, size, shape, composition, and coupling effects, which ought to be synthetically tailored for specific RF excitations. Traditionally, iron oxide NPs (magnetite and/or maghemite) with diameters <15 nm have been used for magnetic fluid hyperthermia. The company MagForce AG (Berl, Germany) utilizes ca. 15-nm iron oxide cores with an amino-silane coating in clinical trials. However, SAR of these NPs is extremely low and, therefore, large doses are required for achieving hyperthermic temperatures in tumors. Employing NPs with optimized SAR values can substantially reduce the required doses, and therefore, many recent works have focused on the development of more efficient magnetic nanoheaters, such as exchange-coupled magnetic NPs (e.g., $\text{CoFe}_2\text{O}_4@ \text{MnFe}_2\text{O}_4$),⁷ iron oxide nanocubes,^{162,163} iron NPs,¹⁶⁴ and iron carbide NPs.¹⁶⁵ Interestingly, magnetosomes produced by magnetotactic bacterium have been reported to produce unusually large SAR values compared to similar magnetic NPs produced by synthetic colloidal methods.^{166,167} This indeed indicates that there is still space for improving synthetic methods to produce more efficient materials.

As was the case for plasmonic heating, most of the reports on magnetic nanoheating involve the destruction of tissue by heating.^{168,169} Many efforts have been devoted to achieving active targeted therapy by functionalization with specific targeting ligands or by using specific cells as Trojan horses.^{41,170,171} Figure 4 shows a classical example of magnetic hyperthermia in which clusters of iron oxide NPs—functionalized with folic acid and polyethylene glycol (PEG) to enhance tumor accumulation—act as nanoheaters and MRI contrast agents.⁴¹ Nevertheless, the most widely used phenomenon toward targeting tumors makes profit of a passive response, i.e., enhanced permeability and retention effect, by which particles typically >100 nm are retained inside tumors due to their characteristic vascularity.¹⁷² Yet, although to a lesser extent than plasmonic heating, other works have attempted to use magnetic heating as a route to promote drug release,¹⁷³ or even targeting of specific cellular receptors, which can be altered by magnetic nanoheating.^{21,174} Figure 5 shows one interesting example of RF-driven smart release.¹⁷⁵ In this work, Aoyagi and coworkers reported a smart hyperthermia nanofiber, which combines heat generation and drug release to induce skin cancer apoptosis.

5.3 Photodynamic Therapy

PDT has been investigated to treat cancers for >100 years.¹⁷⁶ The therapeutic action of PDT relies on the excitation of photosensitizers by light in the presence of oxygen, which enables the production of singlet oxygen in the illuminated areas

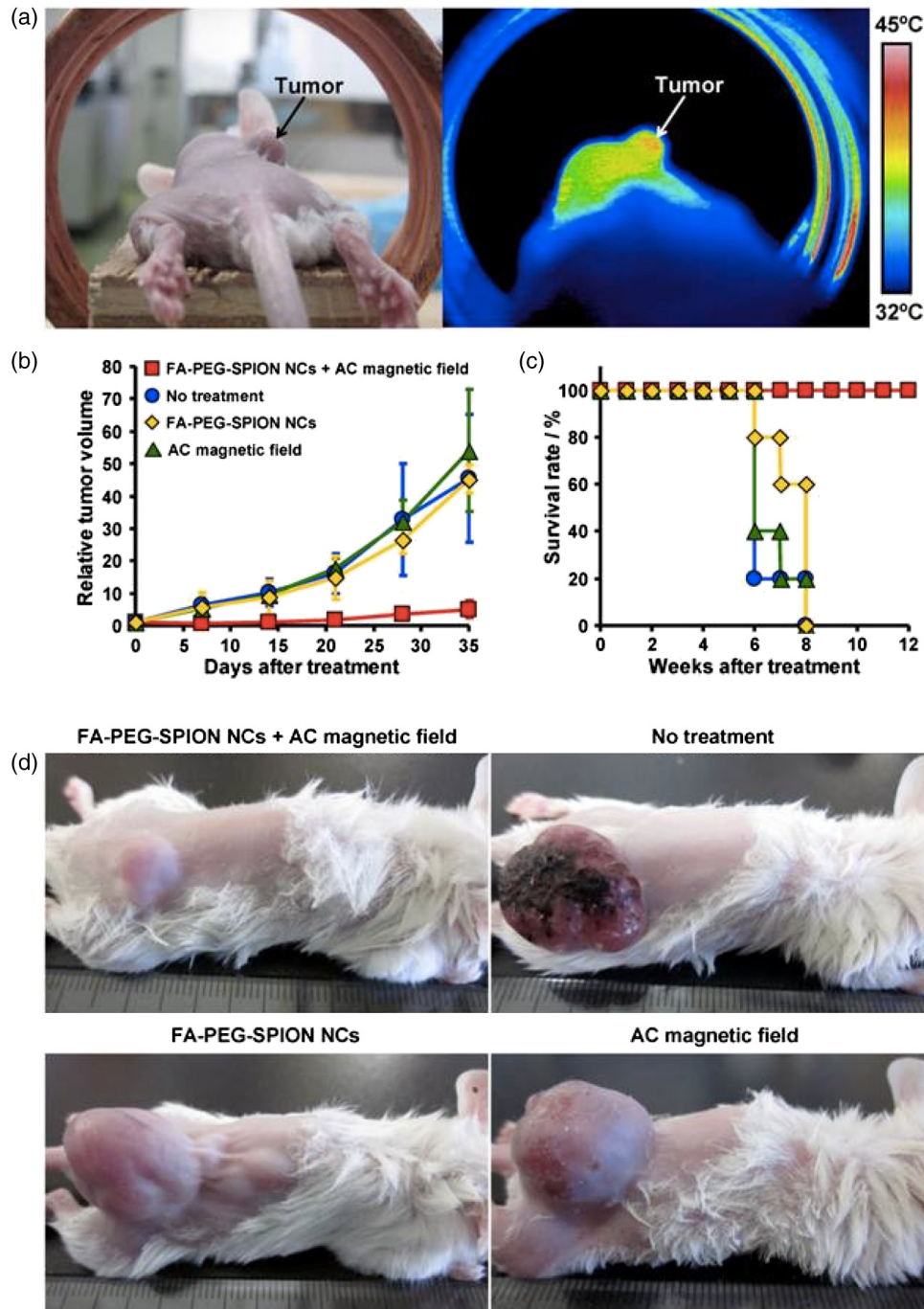


Fig. 4 (a) Photograph (left) and thermal image (right) of a mouse 24 h after intravenous injection of iron oxide agglomerates functionalized with PEG and folic acid [folic acid-polyethylene glycol functionalized superparamagnetic iron oxide nanoparticles (FA-PEG-SPION) nanoclusters (NCs)] under an ac magnetic field with $H = 8$ kA/m and $f = 230$ kHz. (b) Tumor-growth behavior and (c) survival period of mice without treatment and treated by intravenous injection of FA-PEG-SPION NCs, application of an ac magnetic field, and application of an ac magnetic field 24 h after intravenous injection of FA-PEG-SPION NCs ($n = 5$). (d) Photographs of mice 35 days after treatment. Reproduced with permission from Ref. 41.

and, thus, the killing of treated cells. As for plasmonic nanoheating, its therapeutic power resides in the use of light as stimulating triggers for a great degree of spatiotemporal control. Several photosensitizers have been developed,¹⁷⁷ even activatable photosensitizers that require molecular activation, such as quenching, pH, solvent, or hydrophobicity.¹⁷⁸ Also, some hybrid materials that combine photosensitizers and

NPs have been described.^{179–182} In all the above examples, PDT is achieved by direct light excitation of photosensitizers, which may be or may not be tagged on passive NPs, cf. Fig. 3.^{63,183} This review will focus on PDT by EM-active NPs in which reactive oxygen species (ROS) is directly produced by illumination of NPs or by activation of photosensitizers through illumination of NPs.

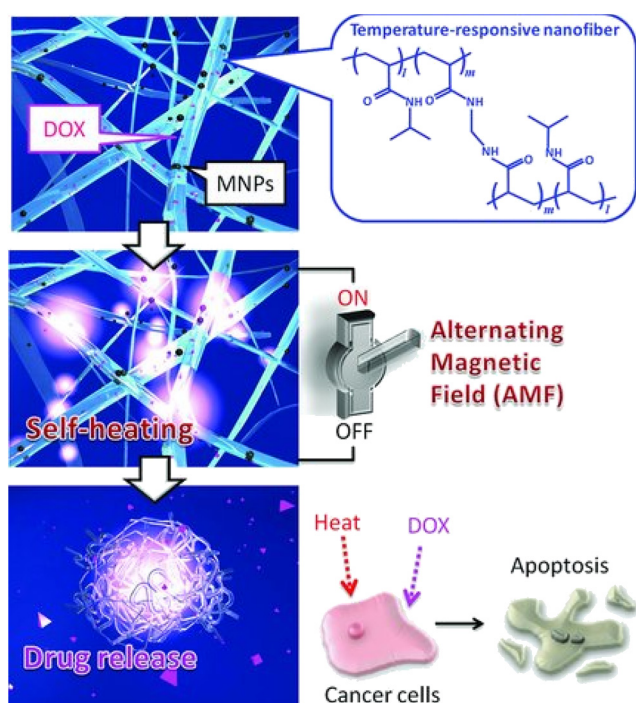


Fig. 5 Design concept for a smart hyperthermia nanofiber system that utilizes magnetic NPs (MNPs) dispersed in temperature-responsive polymers. Anticancer drug doxorubicin (DOX) is also incorporated into the nanofibers. The nanofibers are chemically crosslinked. First, the device signal (AMF) is turned on to activate the MNPs in the nanofibers. Then, the MNPs generate heat to collapse the polymer networks in the nanofiber, allowing the "on-off" release of DOX. Both the generated heat and released DOX induce apoptosis of cancer cells by hyperthermic and chemotherapeutic effects, respectively. Reproduced with permission from Ref. 175.

TiO₂ NPs, a widely used material in consumer products,¹⁸⁴ have been shown to produce ROS upon UV illumination.^{185,186} However, the use of UV light in cytotoxicity studies is rather challenging due to the intrinsic toxicity of UV light. To overcome this, the doping of TiO₂ NPs with different elements has been explored for allowing the TiO₂ NPs' photocatalytic properties into the visible.^{187,188} To date, light activation of TiO₂ NPs represents a major safety concern for nanotoxicology rather than a therapeutic opportunity,¹⁸⁵ although some reports exist.¹⁸⁹⁻¹⁹¹

Equivalent to common photosensitizers, QDs have also been proposed as intrinsic PDT agents.¹⁹²⁻¹⁹⁴ However, the QYs of the singlet oxygen of QDs are very low compared to the ones of common photosensitizers (ca. 1 to 5% versus 20 to 30%). Therefore, most of the reports regarding PDT and QDs describe the use of common photosensitizers in combination with QDs.¹⁹⁵⁻¹⁹⁷ Upon light absorption, photosensitizer-derivatized QDs can produce singlet oxygen. In this case, QDs act as an intermediate of the activation, also known as Förster (fluorescence) resonant energy transfer (FRET) donor. By both one- or two-photon absorption, QDs can be excited with the appropriate light source, and they can subsequently activate photosensitizers, which absorb in the UV-visible. Please notice that the use of PDT has been traditionally limited to surface tumors because usual photosensitizers require low-penetration UV-visible light. Two-photon NIR excitation of photosensitizer-loaded QDs would be highly beneficial for PDT *in vivo*.¹⁹⁸ Both mechanisms, i.e., FRET-based or direct activation of QDs, result in

the generation of reactive singlet oxygen species that can be used for PDT cancer therapy.

On the other hand, the combination of UCNPs and photosensitizers shows great feasibility for cancer treatment, as reported by several works.^{42,77,199-202} UCNPs have been widely used as FRET donors in PDT, which can be activated by NIR light. Photosensitizers are typically embedded in the silica coating of UCNPs, which can undergo energy transfer to the photosensitizers upon NIR excitation, thereby enabling the production of singlet oxygen. Indeed, the unique NIR features of UCNPs make them the ideal platform for PDT. UCNPs solve two of the most important limitations of photosensitizers, i.e., low solubility in aqueous solution and UV-visible activity. Several reports have shown the feasibility of using UCNPs as NIR transducers in PDT *in vivo*.^{42,77,199} The interested reader is referred to the recent work of Arguinzoniz et al., which has covered in detail the most important aspects of PDT driven by NPs.¹⁷⁷

To finish this section, I would like to emphasize that there are many other NP models, EM-active or passive, which can be used for therapeutic purposes though they remain less explored to date. Other therapeutic approaches can also be achieved with the NP models discussed so far. In addition to PDT, for instance, the upconversion phenomenon can be used for NIR-driven release of photocaged compounds.^{34,82} The most common role of NPs in therapy is as drug carriers,²⁰³ which has not been discussed in this review because the therapeutic function of NPs does not rely on the interaction with fields in most of the cases. Therapeutic agents with low solubility (e.g., chemotherapeutic drugs⁷⁴ or photosensitizers²⁰⁴) and/or susceptible to quick degradation (e.g., nucleic acids⁶⁸) can be loaded into NPs with high yield and in combination with other molecules.

6 Nanobiosensing

The capability of EM-active NPs to act as biosensors relies on changes of their physical properties upon analyte recognition, which can be detected by means of a quantifiable optical, thermal, electric, or magnetic signal. Herein, some sound examples of biosensing using EM-active NPs will be discussed. Biosensing using NPs for mass amplification of the signal upon recognition will not be discussed, i.e., microcantilevers or quartz crystal microbalance technology, as in this case, the role of NPs is passive, meaning not active in terms of interaction with fields.

6.1 Optical Readout

The most straightforward and widely used biosensor based on active NPs relies on a change of color (energy resonance), i.e., colorimetric sensors. These have been used to detect the presence of an analyte by simple visual inspection (yes or no sensor), or by spectroscopic means (e.g., plasmon resonance and surface-enhanced Raman). Au and Ag NPs display absorption band(s) in the visible range, which makes them very suitable probes for visual inspection. The plasmon band is mainly determined by the composition, size, and shape of the NPs.² However, changes in the dielectric environment also affect the resonance. This is the basis of localized surface plasmon resonance (LSPR) sensing based on LSPR shifts, where metallic NPs anchored to a substrate produce an LSPR shift upon analyte detection. The most suitable probes are those more sensitive to dielectric changes, such as gold nanorods.²⁰⁵ This technique can be used to detect almost any analyte as long as the colloids are derivatized with catching biomolecules, such as nucleic acids,²⁰⁶

antibodies,^{207–209} carbohydrates,²¹⁰ etc. Figure 6 shows a schematic representation of the basic process of agglomeration, which is caused by the recognition of analytes, and its detection by LSPR.²¹¹ The interested reader in refractometric nanoplasmonic biosensors is referred to two recent reviews from the group of Lechuga.^{212,213}

Yet though LSPR sensing is very versatile, colloidal agglomeration as a colorimetric sensor is extremely sensitive and straightforward, allowing for even naked eye detection. The group of Mirkin has reported pioneering works regarding

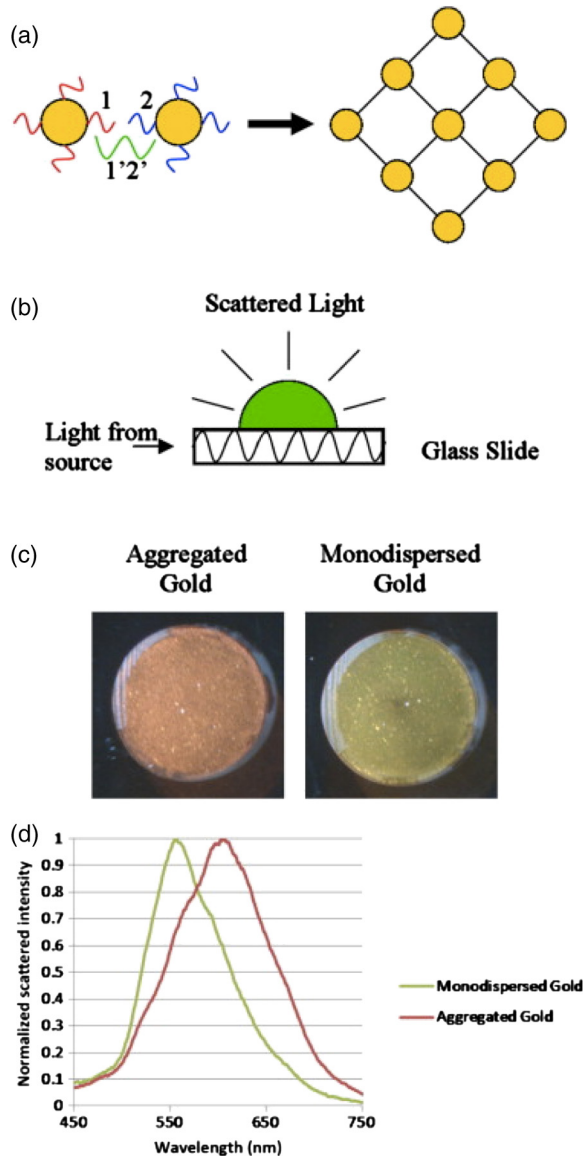


Fig. 6 (a) Schematic representation of the basic process of the analyte-driven agglomeration reaction. Au NPs functionalized with oligonucleotide sequences (Oligo-AuNP conjugates 1 and 2) are bound together into a large agglomerate network by the target sequence 1'2'. (b) Schematic of the principles of the side illumination waveguide system used to illuminate the scattering of the samples. (c) Photograph of representative samples on the side illumination system showing the visible red shift of agglomerated versus monodispersed Au NPs. (d) This shift can also be observed in the localized surface plasmon resonance spectroscopy of the samples. Reproduced with permission from Ref. 211.

colorimetric biosensors based on DNA-modified Au NPs.^{43,69–73,214} The original work describing this concept reports on NP agglomeration (color change) driven by detection of DNA sequences complementary to two DNA-modified Au NPs.²¹⁵ Since this pioneering work, the group of Mirkin has extensively explored the use of ligand-modified Au NPs for biosensing applications. Figure 7 shows one example, which illustrates the versatility and power of this sensing approach, where biobarcode NPs were used for multiplexed detection of protein cancer markers.⁴³

This type of assays has developed into more complex assays, such as colorimetric logic gates.^{216,217} The strength of colorimetric assays relies on the sensitivity of surface plasmons when there is coupling between plasmonic colloids. For instance, dimers of Au NPs (20 nm) with interparticle distances of <10 nm will have a significant impact on the plasmon resonances, both in the cross-section and wavelength.⁶

Another type of optical biosensors is based on FRET. The process requires donor-acceptor pairs in close proximity (1 to 10 nm). Au NPs and QDs have been extensively used in FRET bioassays, the former as donors, which can quench fluorescence of an acceptor due to their high extinction coefficients.²¹⁸ In this way, several different approaches can be used to recover fluorescence upon analyte binding, for example, by using a competitive fluorescence molecule (quenched on the surface of the NP) whereby release occurs (fluorescence recovered) upon analyte detection.²¹⁹ Likewise, plasmonic NPs can be used to enhance the fluorescence of dye molecules placed at ca. 10 nm from the NPs' surface.²²⁰ Actually, fluorescence quenching or enhancement depends on the distance between the NPs and the dye.²²¹ In a recent elegant work on DNA-directed nano-antennas, 117-fold fluorescence enhancement was observed for a dye molecule positioned in the 23-nm gap between 100-nm gold NPs.²²²

In contrast to Au NPs, QDs are typically employed as energy donor molecules in FRET assays. The tunability of QD emission wavelength, large Stokes shifts, and wide absorption spectra enables them to be used as multiplexing agents.^{223–225} As in the case of Au NPs, QDs can be functionalized with biomolecules, which allow for competitive assays or simply analyte recognition whereby the fluorescence is “switch on/off”.²²⁶

Next in this section, basic principles and some examples regarding surface-enhanced Raman scattering (SERS) biosensing are discussed. However, for details about the opportunities and challenges that this ultrasensitive technique can offer, the reader is referred to a recent work of Alvarez-Puebla and coworkers.^{227–230} Briefly, SERS sensing is based on a strong enhancement of the Raman signals upon analyte detection by plasmonic NPs (typically Au and Ag NPs). In principle, this technique can detect single molecules.²³¹ The Raman signal depends strongly on the distance of the Raman reporter to the surface of the NPs, quickly extinguishing as the reporter moves away from the surface. Larger enhancements occur in the gap within agglomerates of NPs, allowing for ultrasensitive sensing. Obviously, between 1- and 2-nm gaps, the range of biomolecules that can fit is very limited. SERS-encoded NPs have been used for multiplex imaging *in vivo*,^{44,232} which could be used for detection of multiple biomarkers associated with a specific disease. The company Oxonica Materials commercializes highly versatile signal-reliable SERS-encoded NPs. These consist of silica-coated agglomerates of Au NPs, which can be encoded with different SERS tags.

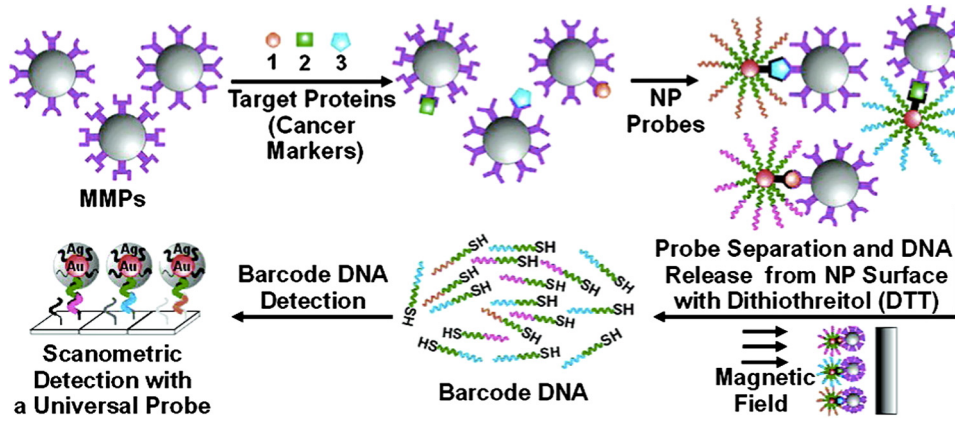


Fig. 7 Biobarcode assay for multiplexed protein detection. Reproduced with permission from Ref. 43.

As an alternative to agglomerates, many investigations have been focused on developing synthetic methods to produce anisotropic plasmonic NPs with sharp apices (nanostars, nanorods, nanoprisms, etc.), which can have hot-spots that concentrate large field enhancements.²³³ By synthetic design, anisotropic plasmonic NPs can be used for energy concentration at the nanoscale. This is actually a fascinating property of plasmonics using EM-active NPs, with many applications besides SERS sensing.²²⁸ Controlled assemblies of plasmonic NPs have been reported to improve SERS sensitivity, whether it is formed by few NPs²³⁴ or by two-dimensional self-assemblies in large supports.²³⁵

Last, photothermal biosensing is briefly introduced. Though the signal is, in this case, thermal, this is achieved due to photoheating using plasmonic NPs. The principle is simple, that is, plasmonic NPs are functionalized with catching biomolecules, which upon recognition immobilize the plasmonic complex in a support. Then, light excitation can produce a thermal signal,

which can be detected by simple visual inspection on a thermo-sensitive support or by a thermal camera.²³⁶ The sensitivity, which can be up to attomolar range in serum of patients,⁴⁵ and the simplicity of this method are astonishing. The principles and protocol of this novel approach are schematically represented in Fig. 8, for the case of detection of a common cancer marker, i.e., carcinoembryonic antigen.⁴⁵

6.2 Magnetic Readout

As in the case of colorimetric biosensors, magnetic NPs can be driven to agglomeration upon analyte recognition, which, in this case, will affect the magnetic relaxation of the surrounding proton spins (as in MRI). As previously mentioned, tailoring the magnetic properties of NPs and, thus, their interaction with RF radiation can be achieved by adjusting the size, shape, and composition of the NPs. This principle can be used to investigate biomolecular interactions, such as DNA-DNA, protein-protein,

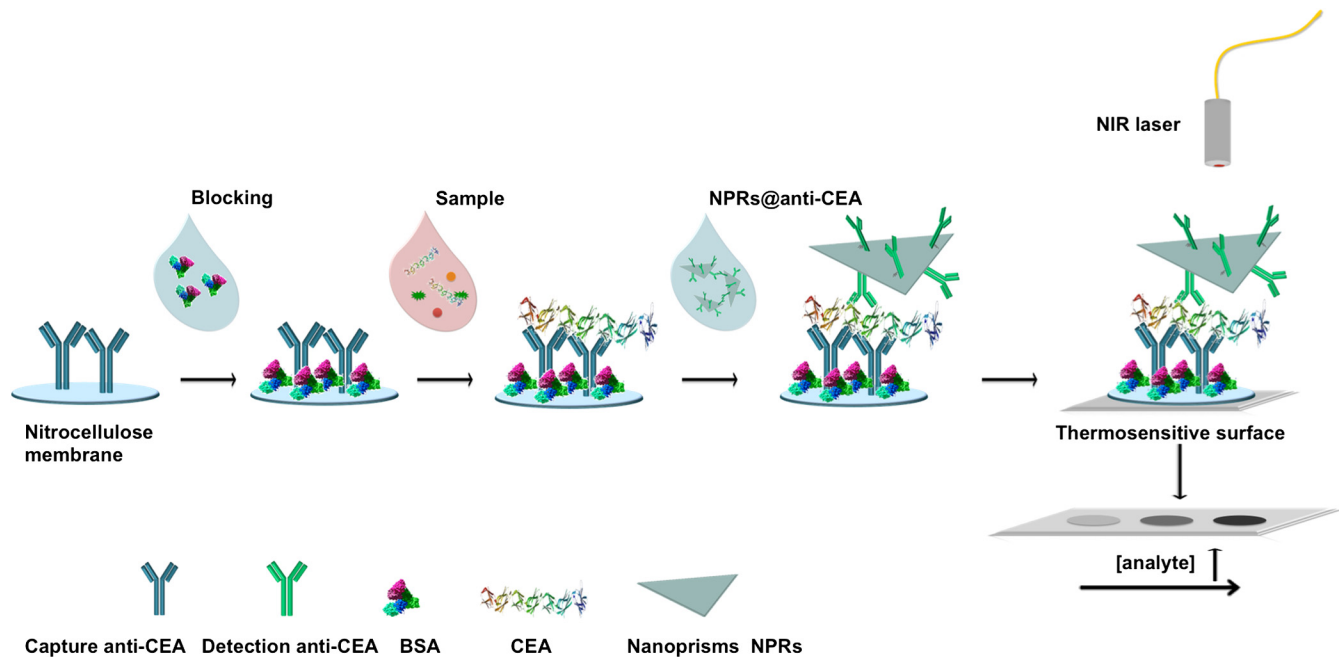


Fig. 8 Schematic representation of thermal biosensing. Step-by-step processes for the formation of the immunocomplex using anti-carcinoembryonic antigen derivatized nanoprism (NPRs), enabling thermal sensing upon near-infrared illumination. Reproduced with permission from Ref. 45.

protein-small molecule, and enzyme reactions.⁴⁶ Importantly, though these measurements require magnetic resonance equipment, which is an obvious disadvantage compared to colorimetric visual inspection, they can be carried out in dirty environments, meaning that sample pretreatment, such as purification, is not required.

6.3 Electric Readout

The electrical detection of target analytes by EM-active NPs, such as CNTs or Au NPs, is based on the measurement of their conductivity and impedance properties upon target recognition. Indeed, CNTs and Au NPs have been widely used as transducers in potentiometric analysis.^{236–238} As in the different sensing methods discussed so far, the most important concept here is that NPs are functionalized with catching molecules, which, upon recognition, change the properties of the transducers. For instance, an aptamer-based CNT potentiometric sensor has been used to detect ultralow concentrations of bacteria.⁴⁸

Another type of electrical sensors is based on the photochemistry of QDs whereby charge carriers can be injected into redox reactions upon light excitation. Thus, current changes depend on whether a reaction occurs, in a quantitative manner, and upon light excitation, which allows one to investigate spatiotemporal-driven reactions.^{47,239,240}

7 Conclusions and Outlook

The applications of NPs in life science are growing dramatically. As the control over the synthesis of complex NPs evolves, new applications and opportunities can be explored. Two main concepts are to be highlighted: first, EM radiation can be absorbed by inorganic NPs, enabling many highly useful responses, like photoluminescence, nanoheating, magnetic coupling, etc. Second, hybrid NPs composed of inorganic EM-active cores and molecules of biological relevance are required for bioperformance enhancement.

Though the field of nanobiotechnology is now in the forefront of science, there are still fundamental issues that have to be deeply addressed, such as the impact of NPs on life, including biocompatibility, toxicity, ecotoxicity, etc.; *in vivo* targeting of specific diseases, markers, etc.; prevention of the unspecific interaction with proteins and accumulation in liver and spleen; and understanding of energy relaxation on NPs and related topics, like hot electrons, magnetic relaxation, heat diffusion in the nanoscale, etc., to mention just few. More work is needed on the development of multifunctional-theranostic NPs, which can perform more than one simple task or serve for more than a proof of principle. As many proof of principles are already established in this area, more efforts should be put into achieving real medical solutions.

References

1. T. K. Sau et al., "Properties and applications of colloidal nonspherical noble metal nanoparticles," *Adv. Mater.* **22**(16), 1805–1825 (2010).
2. L. M. Liz-Marzan, "Tailoring surface plasmons through the morphology and assembly of metal nanoparticles," *Langmuir* **22**(1), 32–41 (2006).
3. A. M. Smith and S. Nie, "Semiconductor nanocrystals: structure, properties, and band gap engineering," *Acc. Chem. Res.* **43**(2), 190–200 (2010).
4. N. Lee and T. Hyeon, "Designed synthesis of uniformly sized iron oxide nanoparticles for efficient magnetic resonance imaging contrast agents," *Chem. Soc. Rev.* **41**(7), 2575–2589 (2012).
5. U. Resch-Genger et al., "Quantum dots versus organic dyes as fluorescent labels," *Nat. Methods* **5**(9), 763–775 (2008).
6. V. Myroshnychenko et al., "Modelling the optical response of gold nanoparticles," *Chem. Soc. Rev.* **37**(9), 1792–1805 (2008).
7. J.-H. Lee et al., "Exchange-coupled magnetic nanoparticles for efficient heat induction," *Nat. Nanotechnol.* **6**(7), 418–422 (2011).
8. A. M. Smith et al., "Bioimaging: second window for *in vivo* imaging," *Nat. Nanotechnol.* **4**(11), 710–711 (2009).
9. N. Kotov, "Bioimaging: the only way is up," *Nat. Mater.* **10**(12), 903–904 (2011).
10. J. K. Streit et al., "Directly measured optical absorption cross sections for structure-selected single-walled carbon nanotubes," *Nano Lett.* **14**(3), 1530–1536 (2014).
11. Y. Du et al., "Near-infrared photoluminescent Ag₂S quantum dots from a single source precursor," *J. Am. Chem. Soc.* **132**(5), 1470–1471 (2010).
12. G. Hong et al., "In vivo fluorescence imaging with Ag₂S quantum dots in the second near-infrared region," *Angew. Chem. Int. Ed.* **51**(39), 9818–9821 (2012).
13. B. Pelaz et al., "Interfacing engineered nanoparticles with biological systems: anticipating adverse nano-bio interactions," *Small* **9**(9–10), 1573–1584 (2013).
14. P. Rivera-Gil et al., "Correlating physico-chemical with toxicological properties of nanoparticles: the present and the future," *ACS Nano* **4**(10), 5527–5531 (2010).
15. D.-E. Lee et al., "Multifunctional nanoparticles for multimodal imaging and theragnosis," *Chem. Soc. Rev.* **41**(7), 2656–2672 (2012).
16. P. del Pino et al., "Protein corona formation around nanoparticles—from the past to the future," *Mater. Horiz.* **1**, 301–313 (2014).
17. P. P. Karmali and D. Simberg, "Interactions of nanoparticles with plasma proteins: implication on clearance and toxicity of drug delivery systems," *Expert Opin. Drug Deliv.* **8**(3), 343–357 (2011).
18. P. Rivera-Gil et al., "The challenge to relate the physicochemical properties of colloidal nanoparticles to their cytotoxicity," *Acc. Chem. Res.* **46**(3), 743–749 (2013).
19. G. Baffou and R. Quidant, "Thermo-plasmonics: using metallic nanostructures as nano-sources of heat," *Laser Photon. Rev.* **7**(2), 171–187 (2013).
20. M. Mahmoudi et al., "Variation of protein corona composition of gold nanoparticles following plasmonic heating," *Nano Lett.* **14**(1), 6–12 (2014).
21. H. Huang et al., "Remote control of ion channels and neurons through magnetic-field heating of nanoparticles," *Nat. Nanotechnol.* **5**(8), 602–606 (2010).
22. C. Hoffmann et al., "Spatiotemporal control of microtubule nucleation and assembly using magnetic nanoparticles," *Nat. Nanotechnol.* **8**(3), 199–205 (2013).
23. C. Hoffmann et al., "Magnetic control of protein spatial patterning to direct microtubule self-assembly," *ACS Nano* **7**(11), 9647–9654 (2013).
24. L. Bonnemay et al., "Engineering spatial gradients of signaling proteins using magnetic nanoparticles," *Nano Lett.* **13**(11), 5147–5152 (2013).
25. N. Erathodiyil and J. Y. Ying, "Functionalization of inorganic nanoparticles for bioimaging applications," *Acc. Chem. Res.* **44**(10), 925–935 (2011).
26. I. Willner and B. Willner, "Biomolecule-based nanomaterials and nanostructures," *Nano Lett.* **10**(10), 3805–3815 (2010).
27. Z. Ali et al., "Multifunctional nanoparticles for dual imaging," *Anal. Chem.* **83**(8), 2877–2882 (2011).
28. V. Bagalkot et al., "Quantum dot-aptamer conjugates for synchronous cancer imaging, therapy, and sensing of drug delivery based on bi-fluorescence resonance energy transfer," *Nano Lett.* **7**(10), 3065–3070 (2007).
29. H. S. Cho et al., "Fluorescent, superparamagnetic nanospheres for drug storage, targeting, and imaging: a multifunctional nanocarrier system for cancer diagnosis and treatment," *ACS Nano* **4**(9), 5398–5404 (2010).
30. N.-H. Cho et al., "A multifunctional core-shell nanoparticle for dendritic cell-based cancer immunotherapy," *Nat. Nanotechnol.* **6**(10), 675–682 (2011).
31. Z. Fan et al., "Multifunctional plasmonic shell-magnetic core nanoparticles for targeted diagnostics, isolation, and photothermal destruction of tumor cells," *ACS Nano* **6**(2), 1065–1073 (2012).
32. M. Dahan et al., "Diffusion dynamics of glycine receptors revealed by single-quantum dot tracking," *Science* **302**(5644), 442–445 (2003).

33. R. Hu et al., "Rational design of multimodal and multifunctional InP quantum dot nanoprobe for cancer: in vitro and in vivo applications," *RSC Adv.* **3**(22), 8495–8503 (2013).
34. Y. Yang et al., "In-vitro and in-vivo uncaging and bioluminescence imaging by using photocaged upconversion nanoparticles," *Angew. Chem. Int. Ed.* **51**(13), 3125–3129 (2012).
35. L. Shang et al., "Ultra-small fluorescent metal nanoclusters: synthesis and biological applications," *Nano Today* **6**(4), 401–418 (2011).
36. K. Kim et al., "Photoacoustic imaging of early inflammatory response using gold nanorods," *Appl. Phys. Lett.* **90**(22), 223901 (2007).
37. C. Bao et al., "Gold nanoprism as photoacoustic signal nanoamplifiers for in vivo bioimaging of gastrointestinal cancers," *Small* **9**(1), 68–74 (2013).
38. J. Y. Park et al., "Paramagnetic ultrasmall gadolinium oxide nanoparticles as advanced T_1 MRI contrast agent: account for large longitudinal relaxivity, optimal particle diameter, and in vivo T_1 MR images," *ACS Nano* **3**(11), 3663–3669 (2009).
39. B. Pelaz et al., "Tailoring the synthesis and heating ability of gold nanoprism for bioapplications," *Langmuir* **28**(24), 8965–8970 (2012).
40. C. M. Hessel et al., "Copper selenide nanocrystals for photothermal therapy," *Nano Lett.* **11**(6), 2560–2566 (2011).
41. K. Hayashi et al., "Superparamagnetic nanoparticle clusters for cancer theranostics combining magnetic resonance imaging and hyperthermia treatment," *Theranostics* **3**(6), 366–376 (2013).
42. N. M. Idris et al., "In vivo photodynamic therapy using upconversion nanoparticles as remote-controlled nanotransducers," *Nat. Med.* **18**(10), 1580–1585 (2012).
43. S. I. Stoeva et al., "Multiplexed detection of protein cancer markers with biobarcode nanoparticle probes," *J. Am. Chem. Soc.* **128**(26), 8378–8379 (2006).
44. C. L. Zavaleta et al., "Multiplexed imaging of surface enhanced Raman scattering nanotags in living mice using noninvasive Raman spectroscopy," *Proc. Natl. Acad. Sci.* **106**(32), 13511–13516 (2009).
45. E. Polo et al., "Plasmonic-driven thermal sensing: ultralow detection of cancer markers," *Chem. Commun.* **49**(35), 3676–3678 (2013).
46. J. M. Perez et al., "Magnetic relaxation switches capable of sensing molecular interactions," *Nat. Biotechnol.* **20**(8), 816–820 (2002).
47. M. Riedel et al., "Photoelectrochemical sensor based on quantum dots and sarcosine oxidase," *Chem. Phys. Chem.* **14**(10), 2338–2342 (2013).
48. G. A. Zelada-Guillén et al., "Immediate detection of living bacteria at ultralow concentrations using a carbon nanotube based potentiometric aptasensor," *Angew. Chem. Int. Ed.* **48**(40), 7334–7337 (2009).
49. I. L. Medintz et al., "Quantum dot bioconjugates for imaging, labelling and sensing," *Nat. Mater.* **4**(6), 435–446 (2005).
50. S. Puertas et al., "Taking advantage of unspecific interactions to produce highly active magnetic nanoparticle-antibody conjugates," *ACS Nano* **5**(6), 4521–4528 (2011).
51. Z. Dai et al., "Nanoparticle-based sensing of glycan-lectin interactions," *J. Am. Chem. Soc.* **128**(31), 10018–10019 (2006).
52. M. Reynolds et al., "Multivalent gold glycoclusters: high affinity molecular recognition by bacterial lectin PA-IL," *Chemistry* **18**(14), 4264–4273 (2012).
53. M. Moros et al., "Monosaccharides versus PEG-functionalized NPs: influence in the cellular uptake," *ACS Nano* **6**(2), 1565–1577 (2012).
54. K. K. Ng et al., "Lipoprotein-inspired nanoparticles for cancer theranostics," *Acc. Chem. Res.* **44**(10), 1105–1113 (2011).
55. Q. Song et al., "Lipoprotein-based nanoparticles rescue the memory loss of mice with Alzheimer's disease by accelerating the clearance of amyloid-beta," *ACS Nano* **8**(3), 2345–2359 (2014).
56. E. C. Dreaden et al., "Tamoxifen-poly(ethylene glycol)-thiol gold nanoparticle conjugates: enhanced potency and selective delivery for breast cancer treatment," *Bioconjug. Chem.* **20**(12), 2247–2253 (2009).
57. M. Das et al., "Intranuclear drug delivery and effective in vivo cancer therapy via estradiol-PEG-appended multiwalled carbon nanotubes," *Mol. Pharm.* **10**(9), 3404–3416 (2013).
58. C. Wang et al., "Drug delivery with upconversion nanoparticles for multi-functional targeted cancer cell imaging and therapy," *Biomaterials* **32**(4), 1110–1120 (2011).
59. F. Sonvico et al., "Folate-conjugated iron oxide nanoparticles for solid tumor targeting as potential specific magnetic hyperthermia mediators: synthesis, physicochemical characterization, and in vitro experiments," *Bioconjug. Chem.* **16**(5), 1181–1188 (2005).
60. C. R. Patra et al., "Fabrication and functional characterization of gold nanoconjugates for potential application in ovarian cancer," *J. Mater. Chem.* **20**(3), 547–554 (2010).
61. G. Zhang et al., "Influence of anchoring ligands and particle size on the colloidal stability and in vivo biodistribution of polyethylene glycol-coated gold nanoparticles in tumor-xenografted mice," *Biomaterials* **30**(10), 1928–1936 (2009).
62. T. Maldiney et al., "Effect of core diameter, surface coating, and PEG chain length on the biodistribution of persistent luminescence nanoparticles in mice," *ACS Nano* **5**(2), 854–862 (2011).
63. J. Lin et al., "Photosensitizer-loaded gold vesicles with strong plasmonic coupling effect for imaging-guided photothermal/photodynamic therapy," *ACS Nano* **7**(6), 5320–5329 (2013).
64. W. Yang et al., "Functionalizable and ultra stable nanoparticles coated with zwitterionic poly(carboxybetaine) in undiluted blood serum," *Biomaterials* **30**(29), 5617–5621 (2009).
65. G. Jia et al., "Novel zwitterionic-polymer-coated silica nanoparticles," *Langmuir* **25**(5), 3196–3199 (2009).
66. P. del Pino et al., "Gene silencing mediated by magnetic lipospheres tagged with small interfering RNA," *Nano Lett.* **10**(10), 3914–3921 (2010).
67. M. Ochs et al., "Light-addressable capsules as caged compound matrix for controlled in vitro release," *Angew. Chem. Int. Ed.* **52**(2), 695–699 (2013).
68. M. E. Davis et al., "Evidence of RNAi in humans from systemically administered siRNA via targeted nanoparticles," *Nature* **464**(7291), 1067–1070 (2010).
69. R. Elghanian et al., "Selective colorimetric detection of polynucleotides based on the distance-dependent optical properties of gold nanoparticles," *Science* **277**(5329), 1078–1081 (1997).
70. J. S. Lee et al., "Colorimetric detection of mercuric ion (Hg^{2+}) in aqueous media using DNA-functionalized gold nanoparticles," *Angew. Chem. Int. Ed.* **46**(22), 4093–4096 (2007).
71. J. M. Nam et al., "Bio-bar-code-based DNA detection with PCR-like sensitivity," *J. Am. Chem. Soc.* **126**(19), 5932–5933 (2004).
72. J. J. Storhoff et al., "One-pot colorimetric differentiation of polynucleotides with single base imperfections using gold nanoparticle probes," *J. Am. Chem. Soc.* **120**(9), 1959–1964 (1998).
73. X. Y. Xu et al., "Colorimetric Cu^{2+} detection using DNA-modified gold-nanoparticle aggregates as probes and click chemistry," *Small* **6**(5), 623–626 (2010).
74. C. Sanson et al., "Doxorubicin loaded magnetic polymersomes: therapeutic nanocarriers for MR imaging and magneto-chemotherapy," *ACS Nano* **5**(2), 1122–1140 (2011).
75. H. Park et al., "Multifunctional nanoparticles for combined doxorubicin and photothermal treatments," *ACS Nano* **3**(10), 2919–2926 (2009).
76. C. M. Copley et al., "Gold nanostructures: a class of multifunctional materials for biomedical applications," *Chem. Soc. Rev.* **40**(1), 44–56 (2011).
77. S. Cui et al., "In vivo targeted deep-tissue photodynamic therapy based on near-infrared light triggered upconversion nanoconstruct," *ACS Nano* **7**(1), 676–688 (2013).
78. P. Zrazhevskiy et al., "Designing multifunctional quantum dots for bioimaging, detection, and drug delivery," *Chem. Soc. Rev.* **39**(11), 4326–4354 (2010).
79. M. Colombo et al., "Biological applications of magnetic nanoparticles," *Chem. Soc. Rev.* **41**(11), 4306–4334 (2012).
80. J. Xie et al., "PET/NIRF/MRI triple functional iron oxide nanoparticles," *Biomaterials* **31**(11), 3016–3022 (2010).
81. E. S. Cho et al., "Ultrasensitive detection of toxic cations through changes in the tunnelling current across films of striped nanoparticles," *Nat. Mater.* **11**(11), 978–985 (2012).
82. Y. Yang et al., "NIR light controlled photorelease of siRNA and its targeted intracellular delivery based on upconversion nanoparticles," *Nanoscale* **5**(1), 231–238 (2013).
83. M. K. G. Jayakumar et al., "Remote activation of biomolecules in deep tissues using near-infrared-to-UV upconversion nanotransducers," *Proc. Natl. Acad. Sci.* **109**(22), 8483–8488 (2012).
84. X.-F. Qiao et al., "Triple-functional core-shell structured upconversion luminescent nanoparticles covalently grafted with photosensitizer for luminescent, magnetic resonance imaging and photodynamic therapy in vitro," *Nanoscale* **4**(15), 4611–4623 (2012).

85. Y. Jin, "Multifunctional compact hybrid Au nanoshells: a new generation of nanoplasmonic probes for biosensing, imaging, and controlled release," *Acc. Chem. Res.* **47**(1), 138–148 (2014).
86. K. Yang et al., "Multimodal imaging guided photothermal therapy using functionalized graphene nanosheets anchored with magnetic nanoparticles," *Adv. Mater.* **24**(14), 1868–1872 (2012).
87. A. Al Zaki et al., "Gold-loaded polymeric micelles for computed tomography-guided radiation therapy treatment and radiosensitization," *ACS Nano* **8**(1), 104–112 (2014).
88. Z. Zhang et al., "Near-infrared light-mediated nanoplatforms for cancer thermo-chemotherapy and optical imaging," *Adv. Mater.* **25**(28), 3869–3880 (2013).
89. D. Boyer et al., "Photothermal imaging of nanometer-sized metal particles among scatterers," *Science* **297**(5584), 1160–1163 (2002).
90. G. Baffou et al., "Thermal imaging of nanostructures by quantitative optical phase analysis," *ACS Nano* **6**(3), 2452–2458 (2012).
91. L. Rodriguez-Lorenzo et al., "Intracellular mapping with SERS-encoded gold nanostars," *Integr. Biol.* **3**(9), 922–926 (2011).
92. J. Moger et al., "Imaging metal oxide nanoparticles in biological structures with CARS microscopy," *Opt. Express* **16**(5), 3408–3419 (2008).
93. Y. Jiang et al., "Bioimaging with two-photon-induced luminescence from triangular nanoplates and nanoparticle aggregates of gold," *Adv. Mater.* **21**(22), 2309–2313 (2009).
94. L. E. Brus, "A simple model for the ionization potential, electron affinity, and aqueous redox potentials of small semiconductor crystallites," *J. Chem. Phys.* **79**(11), 5566–5571 (1983).
95. C. B. Murray et al., "Synthesis and characterization of nearly monodisperse CdE ($E = \text{sulfur, selenium, tellurium}$) semiconductor nanocrystallites," *J. Am. Chem. Soc.* **115**(19), 8706–8715 (1993).
96. A. P. Alivisatos, "Semiconductor clusters, nanocrystals, and quantum dots," *Science* **271**(5251), 933–937 (1996).
97. H. Weller et al., "Photochemistry of semiconductor colloids—properties of extremely small particles of Cd_3P_2 and Zn_3P_2 ," *Chem. Phys. Lett.* **117**(5), 485–488 (1985).
98. M. A. Reed et al., "Observation of discrete electronic states in a zero-dimensional semiconductor nanostructure," *Phys. Rev. Lett.* **60**(6), 535–537 (1988).
99. A. I. Ekimov et al., "Quantum size effect in semiconductor microcrystals," *Solid State Commun.* **56**(11), 921–924 (1985).
100. P. M. Allen and M. G. Bawendi, "Ternary I-III-VI quantum dots luminescent in the red to near-infrared," *J. Am. Chem. Soc.* **130**(29), 9240–9241 (2008).
101. P. M. Allen et al., "InAs(ZnCdS) quantum dots optimized for biological imaging in the near-infrared," *J. Am. Chem. Soc.* **132**(2), 470–471 (2010).
102. T. Pons et al., "Cadmium-free $\text{CuInS}_2/\text{ZnS}$ quantum dots for sentinel lymph node imaging with reduced toxicity," *ACS Nano* **4**(5), 2531–2538 (2010).
103. D. K. Harris et al., "Synthesis of cadmium arsenide quantum dots luminescent in the infrared," *J. Am. Chem. Soc.* **133**(13), 4676–4679 (2011).
104. E. Cassette et al., "Design of new quantum dot materials for deep tissue infrared imaging," *Adv. Drug Delivery Rev.* **65**(5), 719–731 (2013).
105. C. Kirchner et al., "Cytotoxicity of colloidal CdSe and CdSe/ZnS nanoparticles," *Nano Lett.* **5**(2), 331–338 (2005).
106. W. Liu et al., "Compact biocompatible quantum dots via RAFT-mediated synthesis of imidazole-based random copolymer ligand," *J. Am. Chem. Soc.* **132**(2), 472–483 (2010).
107. J. Fan and P. K. Chu, "Group IV nanoparticles: synthesis, properties, and biological applications," *Small* **6**(19), 2080–2098 (2010).
108. V. N. Mochalin et al., "The properties and applications of nanodiamonds," *Nat. Nanotechnol.* **7**(1), 11–23 (2012).
109. A. Magrez et al., "Cellular toxicity of carbon-based nanomaterials," *Nano Lett.* **6**(6), 1121–1125 (2006).
110. F. Wang et al., "Upconversion nanoparticles in biological labeling, imaging, and therapy," *Analyst* **135**(8), 1839–1854 (2010).
111. J.-C. Boyer and F. C. J. M. van Veggel, "Absolute quantum yield measurements of colloidal $\text{NaYF}_4:\text{Er}^{3+}, \text{Yb}^{3+}$ upconverting nanoparticles," *Nanoscale* **2**(8), 1417–1419 (2010).
112. S. H. Yau et al., "An ultrafast look at Au nanoclusters," *Acc. Chem. Res.* **46**(7), 1506–1516 (2013).
113. C. Wang et al., "Near infrared Ag/Au alloy nanoclusters: tunable photoluminescence and cellular imaging," *J. Colloid Interface Sci.* **416**, 274–279 (2014).
114. H.-H. Wang et al., "Fluorescent gold nanoclusters as a biocompatible marker for in vitro and in vivo tracking of endothelial cells," *ACS Nano* **5**(6), 4337–4344 (2011).
115. V. Ntziachristos, "Going deeper than microscopy: the optical imaging frontier in biology," *Nat. Methods* **7**(8), 603–614 (2010).
116. A. De La Zerda et al., "Carbon nanotubes as photoacoustic molecular imaging agents in living mice," *Nat. Nanotechnol.* **3**(9), 557–562 (2008).
117. C. Kim et al., "In vivo molecular photoacoustic tomography of melanomas targeted by bioconjugated gold nanocages," *ACS Nano* **4**(8), 4559–4564 (2010).
118. K. A. Homan et al., "Silver nanoplate contrast agents for in vivo molecular photoacoustic imaging," *ACS Nano* **6**(1), 641–650 (2012).
119. A. Feis et al., "Photoacoustic excitation profiles of gold nanoparticles," *Photoacoustics* **2**(1), 47–53 (2014).
120. N. Lozano et al., "Liposome-gold nanorod hybrids for high-resolution visualization deep in tissues," *J. Am. Chem. Soc.* **134**(32), 13256–13258 (2012).
121. D. A. Nedosekin et al., "Ultra-fast photoacoustic flow cytometry with a 0.5 MHz pulse repetition rate nanosecond laser," *Opt. Express* **18**(8), 8605–8620 (2010).
122. G. Hong et al., "Multifunctional in vivo vascular imaging using near-infrared II fluorescence," *Nat. Med.* **18**(12), 1841–1846 (2012).
123. B. Zhu et al., "Preparation of carbon nanodots from single chain polymeric nanoparticles and theoretical investigation of the photoluminescence mechanism," *J. Mater. Chem. C* **1**(3), 580–586 (2013).
124. F. A. Inam et al., "Emission and nonradiative decay of nanodiamond NV centers in a low refractive index environment," *ACS Nano* **7**(5), 3833–3843 (2013).
125. D. Jurbergs et al., "Silicon nanocrystals with ensemble quantum yields exceeding 60%," *Appl. Phys. Lett.* **88**(23), 233116 (2006).
126. M. Haase and H. Schäfer, "Upconverting nanoparticles," *Angew. Chem. Int. Ed.* **50**(26), 5808–5829 (2011).
127. S. Wang et al., "A 200-fold quantum yield boost in the photoluminescence of silver-doped $\text{Ag}_x\text{Au}_{25-x}$ nanoclusters: the 13th silver atom matters," *Angew. Chem. Int. Ed.* **53**(9), 2376–2380 (2014).
128. B. H. Kim et al., "Large-scale synthesis of uniform and extremely small-sized iron oxide nanoparticles for high-resolution T_1 magnetic resonance imaging contrast agents," *J. Am. Chem. Soc.* **133**(32), 12624–12631 (2011).
129. J. Xiao et al., "Ultrahigh relaxivity and safe probes of manganese oxide nanoparticles for in vivo imaging," *Sci. Rep.* **3**, 3424 (2013).
130. R. Hao et al., "Synthesis, functionalization, and biomedical applications of multifunctional magnetic nanoparticles," *Adv. Mater.* **22**(25), 2729–2742 (2010).
131. P. R. Gil and W. J. Parak, "Composite nanoparticles take aim at cancer," *ACS Nano* **2**(11), 2200–2205 (2008).
132. F. Meng et al., "Intracellular drug release nanosystems," *Mater. Today* **15**(10), 436–442 (2012).
133. A. Boltasseva and H. A. Atwater, "Low-loss plasmonic metamaterials," *Science* **331**(6015), 290–291 (2011).
134. A. M. Alkilany et al., "Gold nanorods: their potential for photothermal therapeutics and drug delivery, tempered by the complexity of their biological interactions," *Adv. Drug Deliv. Rev.* **64**(2), 190–199 (2012).
135. A. M. Javier et al., "Photoactivated release of cargo from the cavity of polyelectrolyte capsules to the cytosol of cells," *Langmuir* **24**(21), 12517–12520 (2008).
136. R. Huschka et al., "Gene silencing by gold nanoshell-mediated delivery and laser-triggered release of antisense oligonucleotide and siRNA," *ACS Nano* **6**(9), 7681–7691 (2012).
137. N. J. Durr et al., "Two-photon luminescence imaging of cancer cells using molecularly targeted gold nanorods," *Nano Lett.* **7**(4), 941–945 (2007).
138. O. Neumann et al., "Compact solar autoclave based on steam generation using broadband light-harvesting nanoparticles," *Proc. Natl. Acad. Sci.* **110**(29), 11677–11681 (2013).
139. A. L. Antaris et al., "Ultra-low doses of chirality sorted (6,5) carbon nanotubes for simultaneous tumor imaging and photothermal therapy," *ACS Nano* **7**(4), 3644–3652 (2013).
140. D. Yoo et al., "Theranostic magnetic nanoparticles," *Acc. Chem. Res.* **44**(10), 863–874 (2011).

141. R. Di Corato et al., "Magnetic nanobeads decorated with silver nanoparticles as cytotoxic agents and photothermal probes," *Small* **8**(17), 2731–2742 (2012).
142. Y. Li et al., "Copper sulfide nanoparticles for photothermal ablation of tumor cells," *Nanomedicine* **5**(8), 1161–1171 (2010).
143. W. Li et al., "CuTe nanocrystals: shape and size control, plasmonic properties, and use as SERS probes and photothermal agents," *J. Am. Chem. Soc.* **135**(19), 7098–7101 (2013).
144. K. Yang et al., "Graphene in mice: ultrahigh in vivo tumor uptake and efficient photothermal therapy," *Nano Lett.* **10**(9), 3318–3323 (2010).
145. S. Lal et al., "Nanoshell-enabled photothermal cancer therapy: impending clinical impact," *Acc. Chem. Res.* **41**(12), 1842–1851 (2008).
146. S. N. Bhatia et al., "Computationally guided photothermal tumor therapy using long-circulating gold nanorod antennas," *Cancer Res.* **69**(9), 3892–3900 (2009).
147. D. P. O'Neal et al., "Photo-thermal tumor ablation in mice using near infrared-absorbing nanoparticles," *Cancer Lett.* **209**(2), 171–176 (2004).
148. R. Huschka et al., "Light-induced release of DNA from gold nanoparticles: nanoshells and nanorods," *J. Am. Chem. Soc.* **133**(31), 12247–12255 (2011).
149. R. Huschka et al., "Visualizing light-triggered release of molecules inside living cells," *Nano Lett.* **10**(10), 4117–4122 (2010).
150. A. Barhoumi et al., "Light-induced release of DNA from plasmon-resonant nanoparticles: towards light-controlled gene therapy," *Chem. Phys. Lett.* **482**(4–6), 171–179 (2009).
151. A. G. Skirtach et al., "Laser-induced release of encapsulated materials inside living cells," *Angew. Chem. Int. Ed.* **45**(28), 4612–4617 (2006).
152. S. J. Leung and M. Romanowski, "Molecular catch and release: controlled delivery using optical trapping with light-responsive liposomes," *Adv. Mater.* **24**(47), 6380–6383 (2012).
153. A. M. Javier et al., "Photoactivated release of cargo from the cavity of polyelectrolyte capsules to the cytosol of cells," *Langmuir* **24**(21), 12517–12520 (2008).
154. S. Carregal-Romero et al., "NIR-light triggered delivery of macromolecules into the cytosol," *J. Control. Release* **159**(1), 120–127 (2012).
155. A.-H. Lu et al., "Magnetic nanoparticles: synthesis, protection, functionalization, and application," *Angew. Chem. Int. Ed.* **46**(8), 1222–1244 (2007).
156. M. Johannsen et al., "Clinical hyperthermia of prostate cancer using magnetic nanoparticles: presentation of a new interstitial technique," *Int. J. Hyperthermia* **21**(7), 637–647 (2005).
157. M. Johannsen et al., "Thermotherapy of prostate cancer using magnetic nanoparticles: feasibility, imaging, and three-dimensional temperature distribution," *Eur. Urol.* **52**(6), 1653 (2007).
158. A. Jordan et al., "Presentation of a new magnetic field therapy system for the treatment of human solid tumors with magnetic fluid hyperthermia," *J. Magn. Magn. Mater.* **225**(1–2), 118–126 (2001).
159. A. Jordan et al., "Magnetic fluid hyperthermia (MFH): cancer treatment with AC magnetic field induced excitation of biocompatible superparamagnetic nanoparticles," *J. Magn. Magn. Mater.* **201**(1–3), 413–419 (1999).
160. A. Jordan et al., "Inductive heating of ferrimagnetic particles and magnetic fluids: physical evaluation of their potential for hyperthermia," *Int. J. Hyperthermia* **9**(1), 51–68 (1993).
161. B. Mehdaoui et al., "Optimal size of nanoparticles for magnetic hyperthermia: a combined theoretical and experimental study," *Adv. Funct. Mater.* **21**(23), 4573–4581 (2011).
162. P. Guardia et al., "Water-soluble iron oxide nanocubes with high values of specific absorption rate for cancer cell hyperthermia treatment," *ACS Nano* **6**(4), 3080–3091 (2012).
163. K. H. Bae et al., "Chitosan oligosaccharide-stabilized ferrimagnetic iron oxide nanocubes for magnetically modulated cancer hyperthermia," *ACS Nano* **6**(6), 5266–5273 (2012).
164. L.-M. Lacroix et al., "Stable single-crystalline body centered cubic Fe nanoparticles," *Nano Lett.* **11**(4), 1641–1645 (2011).
165. A. Meffre et al., "A simple chemical route toward monodisperse iron carbide nanoparticles displaying tunable magnetic and unprecedented hyperthermia properties," *Nano Lett.* **12**(9), 4722–4728 (2012).
166. E. Alphandery et al., "Chains of magnetosomes extracted from AMB-1 magnetotactic bacteria for application in alternative magnetic field cancer therapy," *ACS Nano* **5**(8), 6279–6296 (2011).
167. R. Hergt et al., "Maghemite nanoparticles with very high AC-losses for application in RF-magnetic hyperthermia," *J. Magn. Magn. Mater.* **270**(3), 345–357 (2004).
168. K. Maier-Hauff et al., "Efficacy and safety of intratumoral thermotherapy using magnetic iron-oxide nanoparticles combined with external beam radiotherapy on patients with recurrent glioblastoma multiforme," *J. Neurooncol.* **103**(2), 317–324 (2011).
169. B. Thiesen and A. Jordan, "Clinical applications of magnetic nanoparticles for hyperthermia," *Int. J. Hyperthermia* **24**(6), 467–474 (2008).
170. M.-H. Kim et al., "Magnetic nanoparticle targeted hyperthermia of cutaneous staphylococcus aureus infection," *Ann. Biomed. Eng.* **41**(3), 598–609 (2013).
171. R. S. Rachakatla et al., "Attenuation of mouse melanoma by A/C magnetic field after delivery of bi-magnetic nanoparticles by neural progenitor cells," *ACS Nano* **4**(12), 7093–7104 (2010).
172. A. Fernandez-Fernandez et al., "Theranostic applications of nanomaterials in cancer: drug delivery, image-guided therapy, and multifunctional platforms," *Appl. Biochem. Biotechnol.* **165**(7–8), 1628–1651 (2011).
173. K. Hayashi et al., "High-frequency, magnetic-field-responsive drug release from magnetic nanoparticle/organic hybrid based on hyperthermic effect," *ACS Appl. Mater. Interfaces* **2**(7), 1903–1911 (2010).
174. S. A. Stanley et al., "Radio-wave heating of iron oxide nanoparticles can regulate plasma glucose in mice," *Science* **336**(6081), 604–608 (2012).
175. Y.-J. Kim et al., "A smart hyperthermia nanofiber with switchable drug release for inducing cancer apoptosis," *Adv. Funct. Mater.* **23**(46), 5753–5761 (2013).
176. D. E. J. G. J. Dolmans et al., "Photodynamic therapy for cancer," *Nat. Rev. Cancer* **3**(5), 380–387 (2003).
177. A. G. Arguinoniz et al., "Light harvesting and photoemission by nanoparticles for photodynamic therapy," *Part. Part. Syst. Character.* **31**(1), 46–75 (2014).
178. J. F. Lovell et al., "Activatable photosensitizers for imaging and therapy," *Chem. Rev.* **110**(5), 2839–2857 (2010).
179. P. Huang et al., "Photosensitizer-conjugated magnetic nanoparticles for in vivo simultaneous magnetofluorescent imaging and targeting therapy," *Biomaterials* **32**(13), 3447–3458 (2011).
180. Y. Cheng et al., "Deep penetration of a PDT drug into tumors by non-covalent drug-gold nanoparticle conjugates," *J. Am. Chem. Soc.* **133**(8), 2583–2591 (2011).
181. S. b. Febvay et al., "Targeted cytosolic delivery of cell-impermeable compounds by nanoparticle-mediated, light-triggered endosome disruption," *Nano Lett.* **10**(6), 2211–2219 (2010).
182. T. Stuchinskaya et al., "Targeted photodynamic therapy of breast cancer cells using antibody-phthalocyanine-gold nanoparticle conjugates," *Photochem. Photobiol. Sci.* **10**(5), 822–831 (2011).
183. D. Bechet et al., "Nanoparticles as vehicles for delivery of photodynamic therapy agents," *Trends Biotechnol.* **26**(11), 612–621 (2008).
184. N. A. Monteiro-Riviere et al., "Safety evaluation of sunscreen formulations containing titanium dioxide and zinc oxide nanoparticles in UVB sunburned skin: an in vitro and in vivo study," *Toxicol. Sci.* **123**(1), 264–280 (2011).
185. N. Lu et al., "Nano titanium dioxide photocatalytic protein tyrosine nitration: a potential hazard of TiO₂ on skin," *Biochem. Biophys. Res. Commun.* **370**(4), 675–680 (2008).
186. R. Cai et al., "Induction of cytotoxicity by photoexcited TiO₂ particles," *Cancer Res.* **52**(8), 2346–2348 (1992).
187. T. L. Thompson and J. T. Yates, "Surface science studies of the photoactivation of TiO₂ new photochemical processes," *Chem. Rev.* **106**(10), 4428–4453 (2006).
188. S. George et al., "Role of Fe doping in tuning the band gap of TiO₂ for the photo-oxidation-induced cytotoxicity paradigm," *J. Am. Chem. Soc.* **133**(29), 11270–11278 (2011).
189. S. Yamaguchi et al., "Novel photodynamic therapy using water-dispersed TiO₂-polyethylene glycol compound: evaluation of antitumor effect on glioma cells and spheroids in vitro," *Photochem. Photobiol.* **86**(4), 964–971 (2010).
190. L. Zeng et al., "Multifunctional Fe₃O₄-TiO₂ nanocomposites for magnetic resonance imaging and potential photodynamic therapy," *Nanoscale* **5**(5), 2107–2113 (2013).
191. E. A. Rozhkova et al., "A high-performance nanobio photocatalyst for targeted brain cancer therapy," *Nano Lett.* **9**(9), 3337–3342 (2009).

192. A. C. S. Samia et al., "Semiconductor quantum dots for photodynamic therapy," *J. Am. Chem. Soc.* **125**(51), 15736–15737 (2003).
193. A. Anas et al., "Photosensitized breakage and damage of DNA by CdSe-ZnS quantum dots," *J. Phys. Chem. B* **112**(32), 10005–10011 (2008).
194. S. Dayal et al., "Observation of non-Förster-type energy-transfer behavior in quantum dot-phthalocyanine conjugates," *J. Am. Chem. Soc.* **128**(43), 13974–13975 (2006).
195. J. M. Tsay et al., "Singlet oxygen production by peptide-coated quantum dot-photosensitizer conjugates," *J. Am. Chem. Soc.* **129**(21), 6865–6871 (2007).
196. M. Idowu et al., "Photoinduced energy transfer between water-soluble CdTe quantum dots and aluminium tetrasulfonated phthalocyanine," *New J. Chem.* **32**(2), 290–296 (2008).
197. E. Yaghini et al., "Fluorescence lifetime imaging and FRET-induced intracellular redistribution of Tat-conjugated quantum dot nanoparticles through interaction with a phthalocyanine photosensitizer," *Small* **10**(4), 782–792 (2014).
198. Z.-D. Qi et al., "Biocompatible CdSe quantum dot-based photosensitizer under two-photon excitation for photodynamic therapy," *J. Mater. Chem.* **21**(8), 2455–2458 (2011).
199. C. Wang et al., "Near-infrared light induced in vivo photodynamic therapy of cancer based on upconversion nanoparticles," *Biomaterials* **32**(26), 6145–6154 (2011).
200. D. K. Chatterjee and Z. Yong, "Upconverting nanoparticles as nanotransducers for photodynamic therapy in cancer cells," *Nanomedicine* **3**(1), 73–82 (2008).
201. H. Guo et al., "Singlet oxygen-induced apoptosis of cancer cells using upconversion fluorescent nanoparticles as a carrier of photosensitizer," *Nanomed.: Nanotechnol., Biol. Med.* **6**(3), 486–495 (2010).
202. J. Shan et al., "Pegylated composite nanoparticles containing upconverting phosphors and meso-tetraphenyl porphine (TPP) for photodynamic therapy," *Adv. Funct. Mater.* **21**(13), 2488–2495 (2011).
203. D. Peer et al., "Nanocarriers as an emerging platform for cancer therapy," *Nat. Nanotechnol.* **2**(12), 751–760 (2007).
204. J. P. Celli et al., "Imaging and photodynamic therapy: mechanisms, monitoring, and optimization," *Chem. Rev.* **110**(5), 2795–2838 (2010).
205. C.-D. Chen et al., "Sensing capability of the localized surface plasmon resonance of gold nanorods," *Biosens. Bioelectron.* **22**(6), 926–932 (2007).
206. J. J. Storhoff et al., "Homogeneous detection of unamplified genomic DNA sequences based on colorimetric scatter of gold nanoparticle probes," *Nat. Biotechnol.* **22**(7), 883–887 (2004).
207. K. Fujiwara et al., "Measurement of antibody binding to protein immobilized on gold nanoparticles by localized surface plasmon spectroscopy," *Anal. Bioanal. Chem.* **386**(3), 639–644 (2006).
208. F. Frederix et al., "Biosensing based on light absorption of nanoscaled gold and silver particles," *Anal. Chem.* **75**(24), 6894–6900 (2003).
209. M. Kreuzer et al., "Colloidal-based localized surface plasmon resonance (LSPR) biosensor for the quantitative determination of stanozolol," *Anal. Bioanal. Chem.* **391**(5), 1813–1820 (2008).
210. C. R. Yonzon et al., "A comparative analysis of localized and propagating surface plasmon resonance sensors: the binding of concanavalin A to a monosaccharide functionalized self-assembled monolayer," *J. Am. Chem. Soc.* **126**(39), 12669–12676 (2004).
211. M. S. Cordray et al., "Gold nanoparticle aggregation for quantification of oligonucleotides: optimization and increased dynamic range," *Anal. Biochem.* **431**(2), 99–105 (2012).
212. M. C. Estevez et al., "Trends and challenges of refractometric nanoplasmonic biosensors: a review," *Anal. Chim. Acta* **806**, 55–73 (2014).
213. B. Sepulveda et al., "LSPR-based nanobiosensors," *Nano Today* **4**(3), 244–251 (2009).
214. W. L. Daniel et al., "Colorimetric nitrite and nitrate detection with gold nanoparticle probes and kinetic end points," *J. Am. Chem. Soc.* **131**(18), 6362–6363 (2009).
215. C. A. Mirkin et al., "A DNA-based method for rationally assembling nanoparticles into macroscopic materials," *Nature* **382**(6592), 607–609 (1996).
216. S. Bi et al., "Colorimetric logic gates based on supramolecular DNAzyme structures," *Angew. Chem. Int. Ed.* **49**(26), 4438–4442 (2010).
217. D. Liu et al., "Resettable, multi-readout logic gates based on controllably reversible aggregation of gold nanoparticles," *Angew. Chem. Int. Ed.* **50**(18), 4103–4107 (2011).
218. W. Lihua et al., "Biomolecular sensing via coupling DNA-based recognition with gold nanoparticles," *J. Phys. D: Appl. Phys.* **42**(20), 203001 (2009).
219. W. Zhao et al., "DNA aptamer folding on gold nanoparticles: from colloid chemistry to biosensors," *J. Am. Chem. Soc.* **130**(11), 3610–3618 (2008).
220. H. Li et al., "Silver nanoparticle-enhanced fluorescence resonance energy transfer sensor for human platelet-derived growth factor-BB detection," *Anal. Chem.* **85**(9), 4492–4499 (2013).
221. E. Dulkeith et al., "Gold nanoparticles quench fluorescence by phase induced radiative rate suppression," *Nano Lett.* **5**(4), 585–589 (2005).
222. G. P. Acuna et al., "Fluorescence enhancement at docking sites of DNA-directed self-assembled nanoantennas," *Science* **338**(6106), 506–510 (2012).
223. Y. Xing et al., "Bioconjugated quantum dots for multiplexed and quantitative immunohistochemistry," *Nat. Protoc.* **2**(5), 1152–1165 (2007).
224. S. Carregal-Romero et al., "Multiplexed sensing and imaging with colloidal nano- and microparticles," *Annu. Rev. Anal. Chem.* **6**(1), 53–81 (2013).
225. L. L. del Mercato et al., "Multiplexed sensing of ions with barcoded polyelectrolyte capsules," *ACS Nano* **5**(12), 9668–9674 (2011).
226. A. Coto-García et al., "Nanoparticles as fluorescent labels for optical imaging and sensing in genomics and proteomics," *Anal. Bioanal. Chem.* **399**(1), 29–42 (2011).
227. L. Rodríguez-Lorenzo et al., "Multiplex optical sensing with surface-enhanced Raman scattering: a critical review," *Anal. Chim. Acta* **745**, 10–23 (2012).
228. R. Alvarez-Puebla et al., "Light concentration at the nanometer scale," *J. Phys. Chem. Lett.* **1**(16), 2428–2434 (2010).
229. R. A. Alvarez-Puebla and L. M. Liz-Marzán, "Traps and cages for universal SERS detection," *Chem. Soc. Rev.* **41**(1), 43–51 (2012).
230. R. A. Alvarez-Puebla and L. M. Liz-Marzán, "SERS detection of small inorganic molecules and ions," *Angew. Chem. Int. Ed.* **51**(45), 11214–11223 (2012).
231. E. C. Le Ru et al., "A scheme for detecting every single target molecule with surface-enhanced Raman spectroscopy," *Nano Lett.* **11**(11), 5013–5019 (2011).
232. J. V. Jokerst et al., "Affibody-functionalized gold-silica nanoparticles for Raman molecular imaging of the epidermal growth factor receptor," *Small* **7**(5), 625–633 (2011).
233. S. Barbosa et al., "Tuning size and sensing properties in colloidal gold nanostars," *Langmuir* **26**(18), 14943–14950 (2010).
234. L. Xu et al., "Regiospecific plasmonic assemblies for in situ Raman spectroscopy in live cells," *J. Am. Chem. Soc.* **134**(3), 1699–1709 (2012).
235. S. Gómez-Graña et al., "Self-assembly of Au@Ag nanorods mediated by gemini surfactants for highly efficient SERS-active supercrystals," *Adv. Opt. Mater.* **1**(7), 477–481 (2013).
236. Z. Qin et al., "Significantly improved analytical sensitivity of lateral flow immunoassays by using thermal contrast," *Angew. Chem. Int. Ed.* **51**(18), 4358–4361 (2012).
237. G. A. Crespo et al., "Ion-selective electrodes using carbon nanotubes as ion-to-electron transducers," *Anal. Chem.* **80**(4), 1316–1322 (2008).
238. E. Katz et al., "Electroanalytical and bioelectroanalytical systems based on metal and semiconductor nanoparticles," *Electroanalysis* **16**(1–2), 19–44 (2004).
239. W. Khalid et al., "Immobilization of quantum dots via conjugated self-assembled monolayers and their application as a light-controlled sensor for the detection of hydrogen peroxide," *ACS Nano* **5**(12), 9870–9876 (2011).
240. Z. Yue et al., "Quantum-dot-based photoelectrochemical sensors for chemical and biological detection," *ACS Appl. Mater. Interfaces* **5**(8), 2800–2814 (2013).

Pablo del Pino graduated in physics from Universidad de Sevilla in 2002 and obtained his PhD degree at Technische Universität München, Germany, in 2007. He then joined the group of Wolfgang Parak as a postdoctoral fellow at the Ludwig-Maximilians-Universität München, Munich, Germany. From 2009 to 2013, he was a scientist (first postdoctoral researcher and in 2013, an independent ARAID junior researcher) at Institute of Nanoscience of Universidad de Zaragoza (INA, Zaragoza, Spain). In November 2013, he joined CIC biomaGUNE as senior postdoc in the Biofunctional Nanomaterials unit.